

## Appendix: Solution to problems

### Chapter 2

*Solution 2.1* Using Euler's formula, we can write the sinusoidal signal as the sum of two exponential signals

$$A_i \sin(\omega_0 t) = A_i \cdot \frac{e^{j\omega_0 t} - e^{j(-\omega_0)t}}{2j} \quad (2.1-1)$$

Since we are dealing with a linear system, the output of the sum of the two input signals (here  $A_i \cdot \frac{e^{j\omega_0 t}}{2j}$  and  $-A_i \cdot \frac{e^{j(-\omega_0)t}}{2j}$ ) equals the sum of the individual output signals. These are

$$A_i \frac{e^{j\omega_0 t}}{2j} \cdot |T(j\omega_0)| \cdot e^{j\Phi(\omega_0)} \quad \text{and} \quad -A_i \frac{e^{j(-\omega_0)t}}{2j} \cdot |T(j(-\omega_0))| \cdot e^{j\Phi(-\omega_0)}, \text{ respectively.}$$

Therefore, the complete filter output signal is equal to:

$$A_i \frac{(|T(j\omega_0)| \cdot e^{j\Phi(\omega_0)})e^{j\omega_0 t} - (|T(j(-\omega_0))| \cdot e^{j\Phi(-\omega_0)})e^{j(-\omega_0)t}}{2j} \quad (2.1-2)$$

Because  $|T(j(-\omega_0))| = |T(j\omega_0)|$  for the RC-filter (and for any real filter), we obtain

$$A_i \frac{|T(j\omega_0)|}{2j} (e^{j\omega_0 t + j\Phi(\omega_0)} - e^{j(-\omega_0)t + j\Phi(-\omega_0)}) \quad (2.1-3)$$

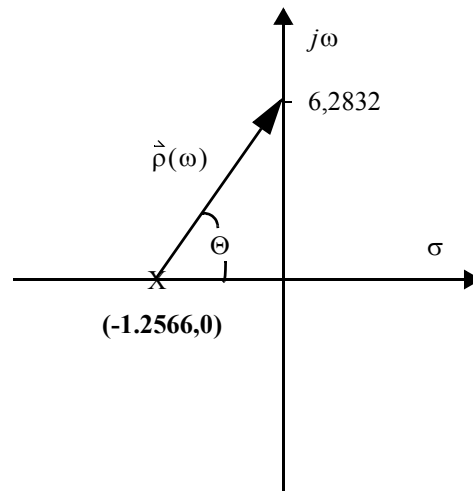
Since  $\Phi(\omega_0) = \text{atan}(\text{Im}(T(j\omega_0))/\text{Re}(T(j\omega_0)))$  and  $\text{atan}(-\alpha) = -\text{atan}(\alpha)$  we obtain  $\Phi(-\omega_0) = -\Phi(\omega_0)$  and the output signal becomes

$$\begin{aligned} A_i \cdot \frac{|T(j\omega_0)|}{2j} (e^{j(\omega_0 t + \Phi(\omega_0))} - e^{-j(\omega_0 t + \Phi(\omega_0))}) \\ = A_i \cdot |T(j\omega_0)| \cdot \sin(\omega_0 t + \Phi(\omega_0)) \end{aligned} \quad (2.1-4)$$

Using equations (2.21) and (2.22) we obtain for the RC filter output

$$A_i \cdot \frac{1}{\sqrt{1 + (RC\omega_0)^2}} \sin(\omega_0 t - \text{atan}(\omega_0 RC)) \quad (2.1-5)$$

**Solution 2.2** The pole position is at  $-1/\tau$ .  $\tau = R \cdot C = 4,0\Omega \cdot 0,1989495F$  which is  $4,0V/A \cdot 0,1989495A \text{ sec}/V = 0,795798 \text{ sec}$ . Hence, the pole is at  $-1,2566$  (rad/s). For each point on the imaginary axis (angular frequency axis), determine the reciprocal of the length of the vector from the pole to that point. You can do this either by using a ruler and graph paper or simply by exploiting analytical geometry. Plot this value as a function of angular frequency or frequency, respectively. Below, the procedure is demonstrated schematically for a frequency of 1Hz (Fig. A 2.1; note, that Fig. A 2.1 is not on 1:1 scale).



**Example: f=1 Hz**

$$\omega = 2\pi \cdot 1 = 6,2832$$

$$|\vec{p}(2\pi)| = 6,4076$$

$$|T(j2\pi)| = \frac{1}{\tau} \left[ \frac{1}{|\vec{p}(\omega)|} \right]$$

$$|T(j2\pi)| = \frac{1,2566}{6,4076} = 0,1961$$

**Fig. A 2.1** Graphical determination of the modulus of the frequency response function for the RC filter of Problem 2.2. The plot demonstrates the evaluation for a frequency of 1 Hz.

*Solution 2.3* The Digital Seismology Tutor (DST) simulates the action of systems defined by their transfer function in the complex s-plane. As we will see later in more detail, a transfer function of a more general system can have more than one pole as well as a number of zeros (at which the transfer function becomes zero). The positions of poles and zeros define the transfer function completely. In order to do the filtering, DST needs to know the position(s) of the pole(s) and zero(s) (which will be introduced in later chapters) in the complex s-plane.

After starting up the DST, select the *Modify and Enter* option from the *Poles/Zeros* menu. In order to enter the pole position for the RC-filter at  $(-1.2566, 0)$ , enter the real part  $(-1.2566)$  into the uppermost left box and the imaginary part  $(0.0)$  into the uppermost right box as shown in Fig. A 2.2. Enter a 1.0 for the scale factor in the bottom box. Finally accept the input either by using the *OK* or the *Apply* button. The difference between these two is merely that the *OK* button closes the window after accepting the input while the *Apply* button leaves is open for further input.

POLES	
real part	-1.2566
imaginary part	0

ZEROS	
real part	
imaginary part	

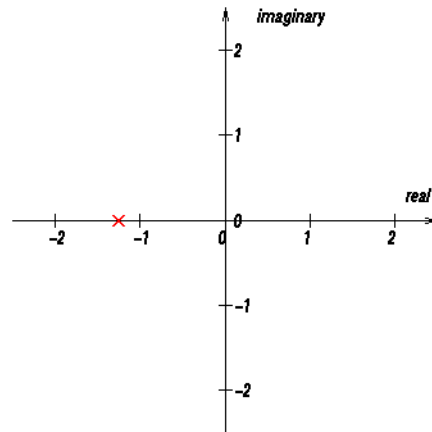
  

Scale Factor
1.0

Ok Apply Reset Cancel

**Fig. A 2.2** How to enter the pole position for Problem 2.3 into the *Modify and Enter Poles/Zero* panel of the DST.

After you entered the pole into the DST, you can visualize its position within the complex s-plane by using the *Map* option from the *Poles/Zeros* menu (Fig. A 2.3).



**Fig. A 2.3** Pole position of RC-filter from Problem 2.3 within the complex s-plane as calculated with DST.

The corresponding frequency response can be viewed using the *Show Response* menu from the DST main window using the option *Frequency Response -> Amplitude-> lin-lin* (Fig. A 2.4).

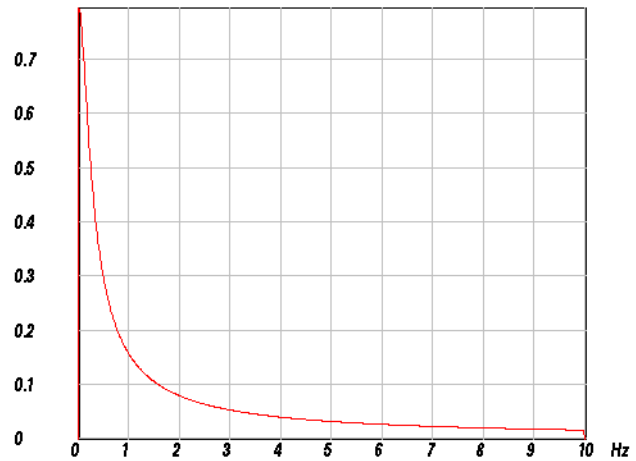


**Fig. A 2.4** Frequency response function (amplitude only) for the pole position shown in Fig. A 2.3.

**Note:** Although the plot in Fig. A 2.4 shows a continuous curve, it is actually a discrete approximation of the continuous frequency response function. The details of the underlying relationship will be explained in detail in chapter 7 “From infinitely continuous to

finite discrete”. At this point it is sufficient to know that the internal sampling frequency for the calculation of the frequency response function can be modified in the *Setup* menu. For reasons which are explained in chapter 7, the frequency band which is plotted ranges from 0 to 1/2 of the internal sampling frequency.

*Solution 2.4* The balance at time  $t = nT + T$ :

$$y(nT + T) = y(nT) + \alpha y(nT) + \alpha x(nT) + x(nT) \quad (2.4-1)$$

$$= y(nT) + \alpha y(nT) + (\alpha + 1) \cdot x(nT) \quad (2.4-2)$$

$$y(nT + T) - y(nT) = \alpha y(nT) + (\alpha + 1) \cdot x(nT) \quad (\text{divide by } T) \quad (2.4-3)$$

$$\frac{y(nT + T) - y(nT)}{T} = \frac{\alpha}{T} y(nT) + \frac{(\alpha + 1)}{T} \cdot x(nT) \quad (2.4-4)$$

Next, replace the difference quotient by the derivative and  $nT$  by  $t$ :

$$\dot{y}(t) - \frac{\alpha}{T} y(t) = \frac{(\alpha + 1)}{T} \cdot x(t) \quad (2.4-5)$$

Taking the Laplace transform yields

$$s \cdot Y(s) - \frac{\alpha}{T} \cdot Y(s) = \frac{\alpha + 1}{T} \cdot X(s) \quad (2.4-6)$$

$$\left(s - \frac{\alpha}{T}\right) \cdot Y(s) = \frac{\alpha + 1}{T} \cdot X(s) \quad (2.4-7)$$

$$T(s) = \frac{Y(s)}{X(s)} = \frac{\alpha + 1}{T} \cdot \frac{1}{s - \frac{\alpha}{T}} \quad (2.4-8)$$

From the equation above we see that a pole exists at  $s = \alpha / T$

The corresponding impulse response becomes:  $\frac{\alpha + 1}{T} \cdot e^{\frac{\alpha}{T} \cdot t}$

From the positive exponent we see that the impulse response is unstable! While this is normally an unwanted feature, for a checking account it is just what we expect!

### Chapter 3

**Solution 3.1** In order to obtain an internal sampling frequency of 100 Hz and a window length of 2048 points as recommended in Problem 3.1, these values have to be entered into the *Setup* menu (*Modify* option). For the spike position of the impulse response enter a value of 1024 to obtain a centered spike. To finally accept the input, you have to use either the *OK* or the *Accept* button. For part a) select the *Modify and Enter* option from the *Poles/Zeros* menu and enter the real and imaginary parts of each pole position on a separate line of the uppermost input boxes as shown in Fig. A 3.1.

The figure shows a software interface for entering pole and zero data. It is divided into two main sections: **POLES** and **ZEROS**. Each section has two input fields: *real part* and *imaginary part*. In the **POLES** section, the *real part* field contains the values  $-1.2566$  and  $-1.2566$  on two separate lines, and the *imaginary part* field contains  $0.0$  and  $0.0$  on two separate lines. The **ZEROS** section has empty input fields. Below these sections is a *Scale Factor* field containing the value  $1.0$ . At the bottom, there are four buttons: *Ok*, *Apply*, *Reset*, and *Cancel*.

**Fig. A 3.1** Pole/Zero input panel for Problem 3.1a).

The corresponding impulse response function can be viewed using the *Impulse Response* option from the *Show Response* menu of the DST (Fig. A 3.2).



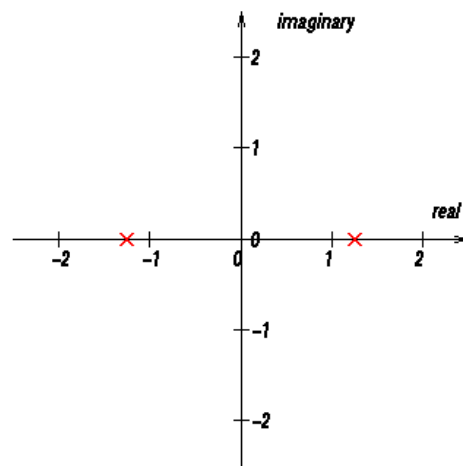
**Fig. A 3.2** Impulse response function for Problem 3.1a).

For Problem 3.1b), one pole falls into the left half of the s-plane while the other is located in the right half. The input for the corresponding pole positions is shown in Fig. A 3.3.

The figure shows a software interface for defining pole and zero positions. It is divided into two main sections: 'POLES' and 'ZEROS'. Each section contains two input fields: 'real part' and 'imaginary part'. In the 'POLES' section, the 'real part' field contains the value -1.2566 and the 'imaginary part' field contains 0.0. The 'ZEROS' section has empty input fields. Below these sections is a 'Scale Factor' field with the value 1.0. At the bottom are four buttons: 'Ok', 'Apply', 'Reset', and 'Cancel'.

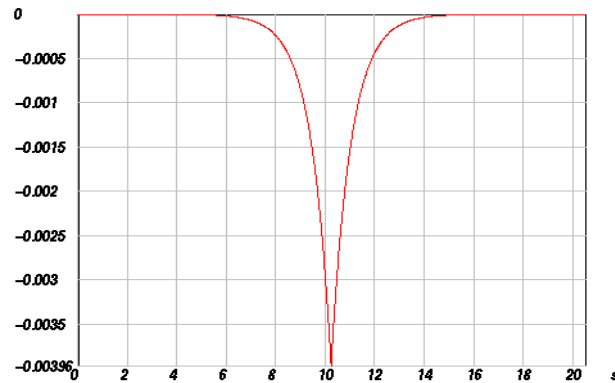
**Fig. A 3.3** Pole position input panel for Problem 3.1b).

Fig. A 3.4 displays the corresponding pole map (option *Map* from the *Poles/Zeros* menu).



**Fig. A 3.4** Pole map for Problem 3.1b).

The resulting impulse response shows a signal symmetric to the position of the input spike Fig. A 3.5.



**Fig. A 3.5** Impulse response function for Problem 3.1b).

Finally, if the two poles are both put into the right half  $s$ -plane - Problem 3.1c) - the resulting impulse response function is a left-sided signal as shown in Fig. A 3.6.

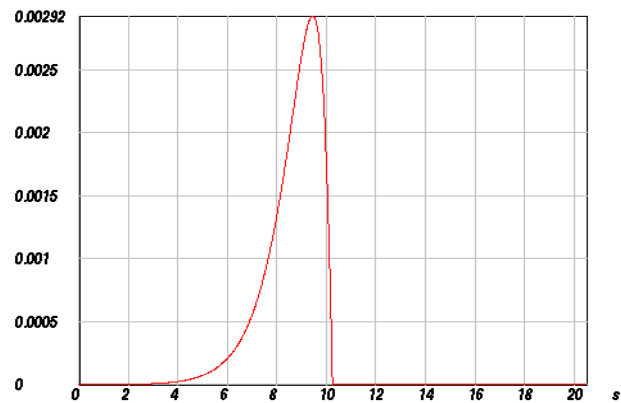


**Fig. A 3.6** Impulse response function for Problem 3.1c).

Hence, the resulting impulse response function will be a) right-sided, b) two-sided, and c) left sided which can be understood from the arguments in chapter 3.1. The amplitude portion of the frequency response function is identical in all three cases while the phase response differs.

With respect to Problem 2.3, the slope of the amplitude response is steeper by 20dB/decade since an additional pole is present.

**Solution 3.2** Since the pole and the zero become symmetrical to the imaginary axis, the pole vectors and zero vectors are always of equal length. Hence their ratio is always constant. It follows that the amplitude response is the same for all frequencies, characteristic of an allpass filter. Fig. A 3.7 shows the pole/zero distribution (a) and the corresponding impulse response function (b).

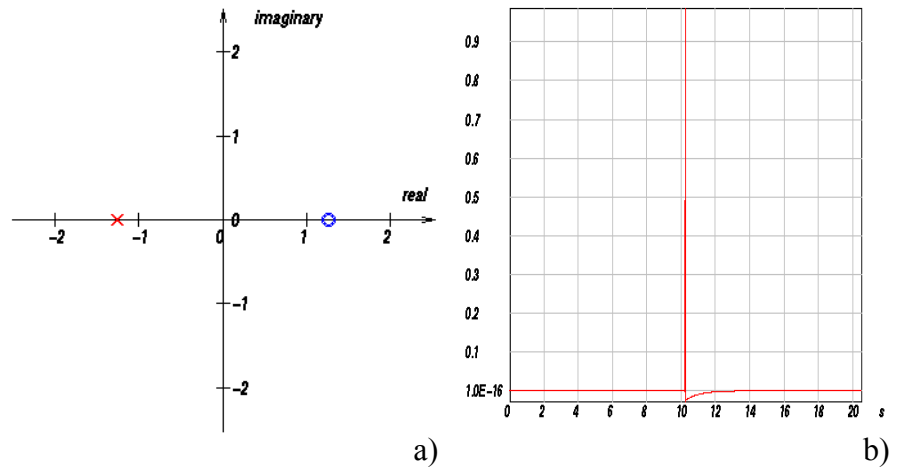


**Fig. A 3.7** a) Pole/zero distribution and b) input impulse function of the allpass filter of Problem 3.2. The amplitude part of the frequency response is constant for all frequencies (not shown).

**Solution 3.3** a) A general transfer function  $F(s)$  will be described by poles and zeros. Taking the inverse,  $1/F(s)$  causes all poles to become zeros and zeros to become poles. For a minimum phase system, all the poles and zeros of the transfer function  $F(s)$  are on the left half s-plane. This will not change for the inverse system. Hence, the inverse system will also be minimum phase and therefore stable. b) The poles and zeros of a general mixed phase system with zeros on either half-plane can always be expanded into two systems. The allpass is constructed by taking all right half-plane zeros and adding symmetric poles. The minimum phase system is constructed by taking all poles (which have to be in the left half-plane anyway for stability reasons) and adding zeros where the allpass system had added poles for symmetry reasons. On multiplication of the two transfer functions these additional poles and zeros will cancel (Fig. A 3.8).

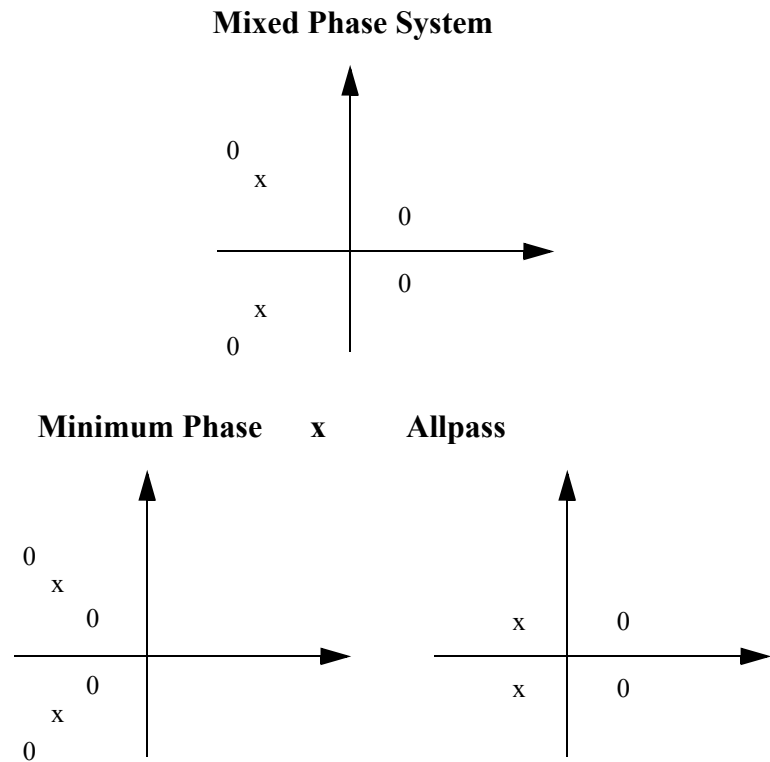


**Fig. A 3.8** Separating a mixed phase system into a minimum phase system and an allpass.

*Solution 3.4* Since the transfer function for Problem 3.1b has a pole on either side of the imaginary axis, we need to cancel the right-sided pole by a zero. In order not to change the amplitude characteristic, we have to do this with an allpass filter whose poles and zeros are symmetrical to the imaginary axis. The filter we need must have a zero at  $(+1.2566, 0)$  and a pole at  $(-1.2566, 0)$ , which is exactly the allpass from Problem 3.2. The poles and zeros of the filter have to be added to the poles and zeros of the original system. Therefore, the filtered system will have two poles at  $(-1.2566, 0)$ , one at  $(1.2566, 0)$ , and a zero at  $(1.2566, 0)$  as shown in Fig. A 3.9.

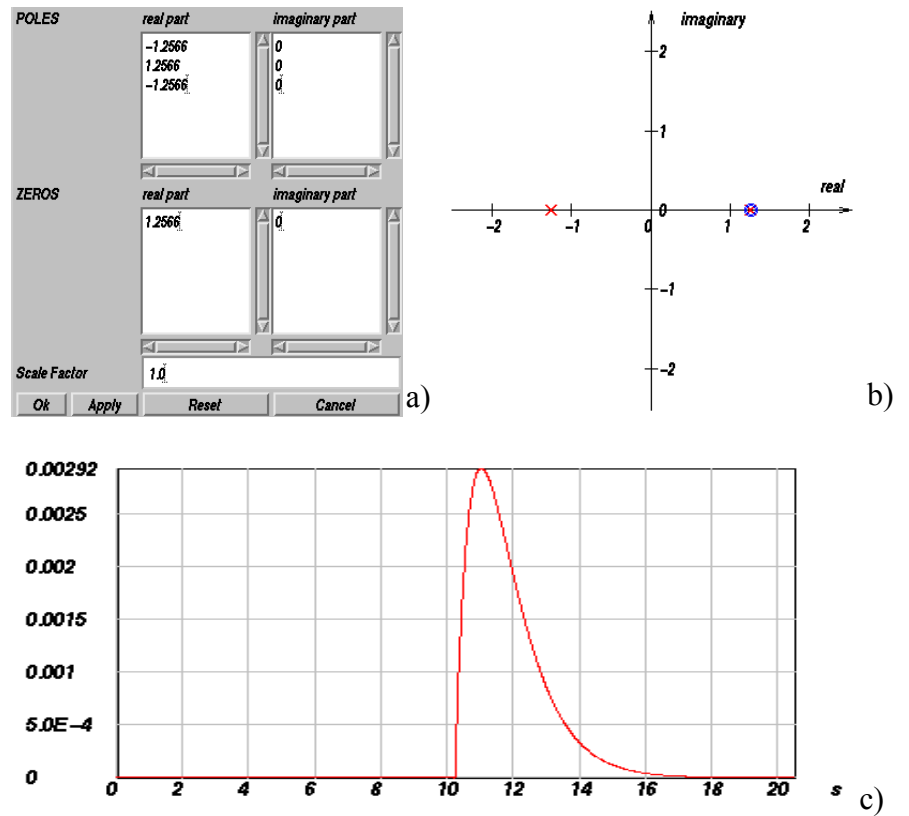


**Fig. A 3.9** Poles and Zeros input menu in DST (a), corresponding poles and zeros map (b), and impulse response function of the filtered system of Problem 3.1b (c). The internal sampling frequency in DST was set to 100 Hz (*Setup* menu).

*Solution 3.5* For this exercise, an internal sampling frequency of 20 Hz is recommended (*Modify* option in the *Setup* menu) in DST. First, select the *Modify and Enter* option from the *Poles/Zeros* menu and enter the real and imaginary parts of the pole and zero position. Fig. A 3.10 displays the pole/zero map and the amplitude part of the corresponding frequency response function.

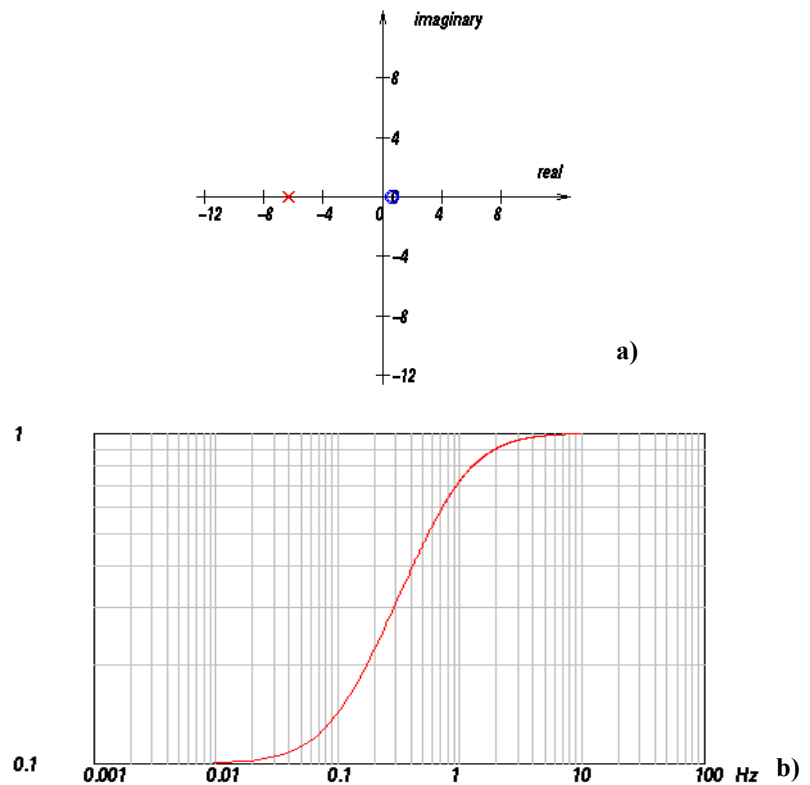


**Fig. A 3.10** Pole/zero map (a) and amplitude part of the frequency response function (b) for a system consisting of a pole at  $(-6.28318, 0.0)$  and a zero at  $(0.628318, 0.0)$ . Fig. A 3.10 was created using DST with an internal sampling frequency of 20 Hz and 2048 points for the FFT (*Setup* menu).

From the pole and zero positions we expect corner frequencies at  $f_1 = 0.1$  Hz and at  $f_2 = 1$  Hz, respectively. We can see that the frequency response function starts out constant, increases by 20 dB/decade at  $f_1$  then decreases by 20 dB/decade at  $f_2$ .

*Solution 3.6* Start out with the double pole at  $(-1.2566, 0)$ . For the successive steps, the pole positions would be  $p_{1,2} = -1.2566(\cos\alpha + j\sin\alpha)$  with  $\alpha$  being incremented from  $15^\circ$  to  $75^\circ$  in steps of  $15^\circ$  (plus  $\alpha = 85^\circ$ ,  $\alpha$  is measured clockwise from the negative real s-axis).

The corresponding pole positions are given below:

$[\text{ }^\circ]$	pole position
$0^\circ$	$-1,2566 \pm j0,0$
$15^\circ$	$-1,21378 \pm j0,325232$
$30^\circ$	$-1,08825 \pm j0,6283$
$45^\circ$	$-0,88855 \pm j0,88855$
$60^\circ$	$-0,6283 \pm j1,08825$
$75^\circ$	$-0,325232 \pm j1,21378$
$85^\circ$	$-0,10952 \pm j1,25182$

Below, the resulting impulse response functions are shown for  $30^\circ$ ,  $60^\circ$ , and  $85^\circ$  (Fig. A 3.11 - Fig. A 3.13).

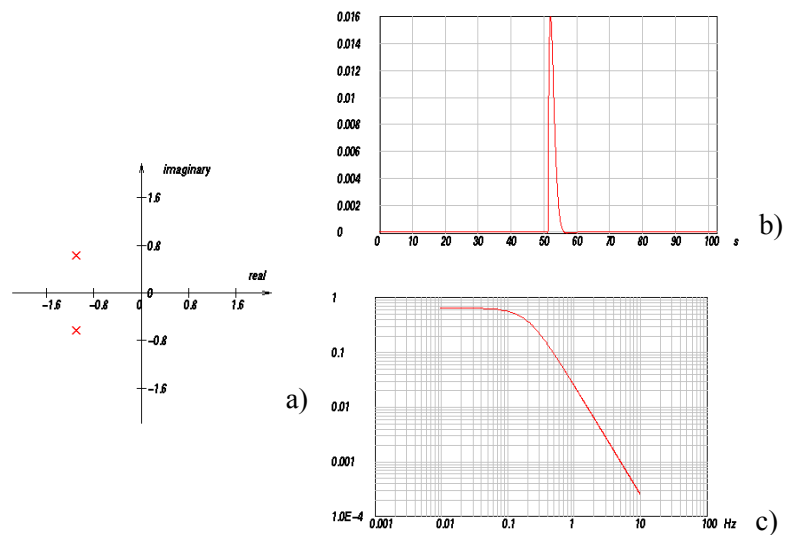


**Fig. A 3.11** Pole positions (a), impulse response (b) and frequency response (c) for a system with a conjugate complex pole pair with the pole positions at an angle of  $30^\circ$  from the real axis of the s-plane. The internal sampling frequency in DST was 20 Hz, the window length 2048 points, and the spike position for the impulse response 1024 (*Setup* menu).

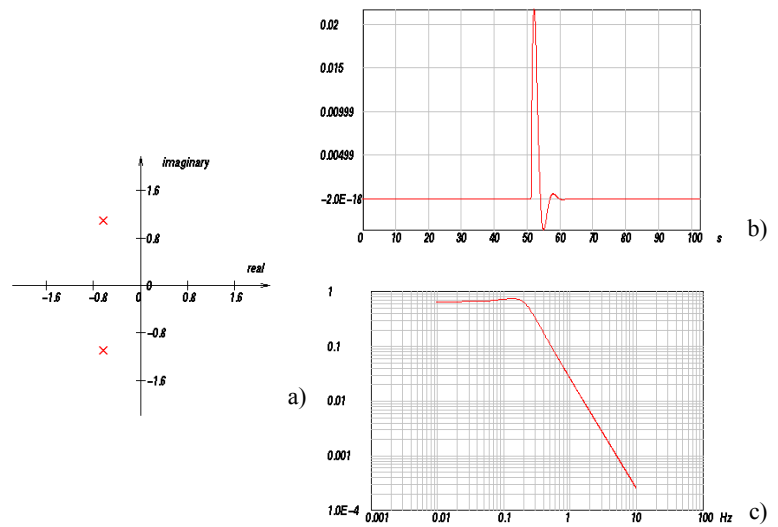


**Fig. A 3.12** Pole positions (a), impulse response (b), and frequency response (c) for a system with a conjugate complex pole pair with the pole positions at an angle of  $60^\circ$  from the real axis of the s-plane.

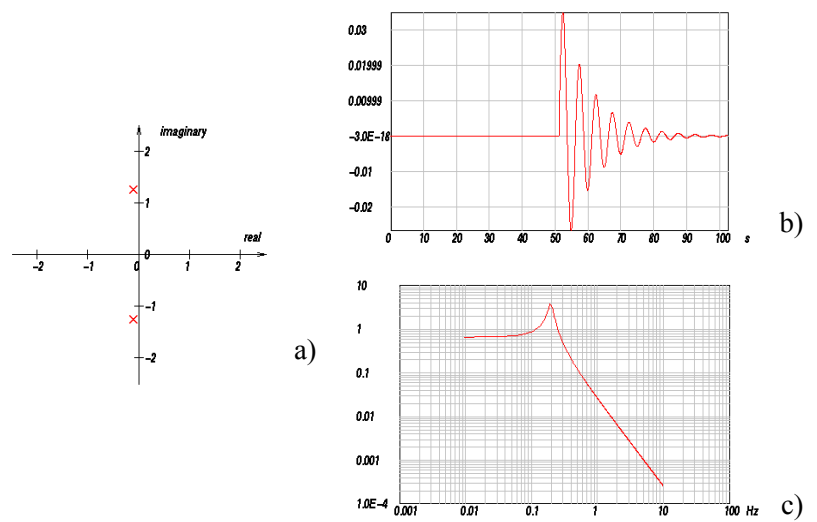


**Fig. A 3.13** Pole positions (a), impulse response (b), and frequency response (c) for a system with a conjugate complex pole pair with the pole positions at an angle of  $85^\circ$  from the real axis of the s-plane.

As the poles get closer to the imaginary axis, there are more oscillations in the impulse response. On the other hand when the poles are farther from the imaginary axis, the oscillations are more strongly damped. Notice that the spectrum changes significantly only near the corner frequency, not at the high and low ends of the spectrum.

*Solution 3.7* In Problem 3.6 we have seen that the amplitude part of the frequency response functions shows a strong peak if the poles were close to the imaginary axis. Hence, zeros close to the imaginary axis will correspond to strong selective suppression which is what we need. Therefore, we need to put zeros on or very close to the imaginary axis. In order to sharpen the notch, we also have to put poles close to the zeros, canceling their effect for frequencies away from the notch frequency. One solution is shown below (Fig. A 3.14).

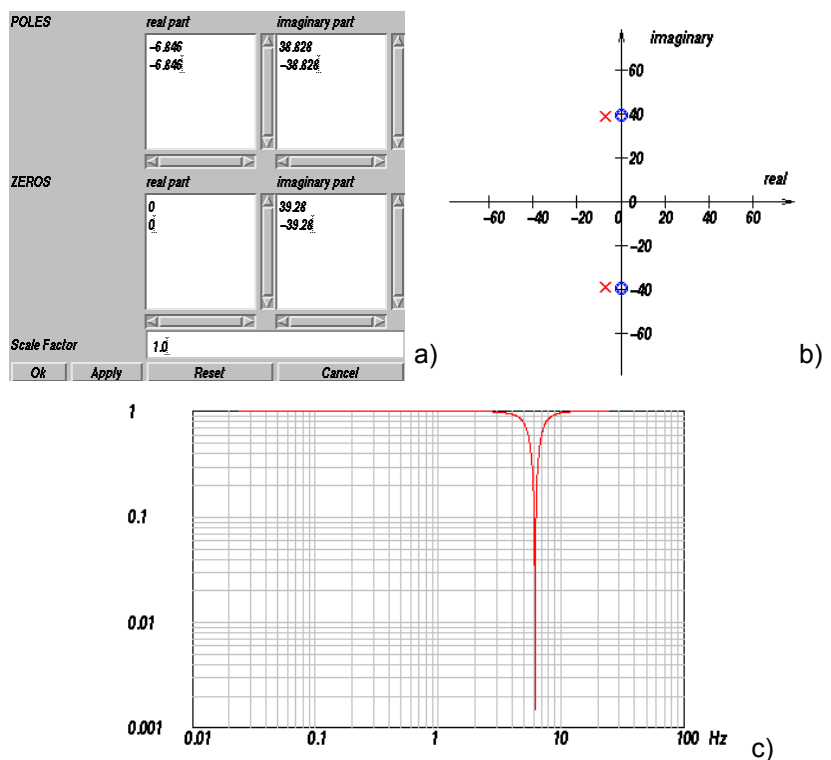


**Fig. A 3.14** Poles and Zeros input menu in DST (a), corresponding poles/zeros map (b), and amplitude frequency response function for a notch filter at 6.25 Hz. The corner frequency corresponding to the chosen pole position was 6.275 Hz, the corner frequency corresponding to the chosen zero positions 6.25 Hz. The internal sampling frequency in DST was 20 Hz, the window length 2048 points, and the spike position for the impulse response 1024 (*Setup* menu).

**Solution 3.8** Within DST, the frequency response function of Problem 3.8 can be modeled by poles and zeros entered via the *Modify and Enter* option of the *Poles/Zeros* menu. First select *problem3.8* from the *Load Response to Fit* option of the *Poles/Zeros* menu to display the frequency response function shown in Fig. 3.4. Next, estimate the different slopes and determine the number of poles and zeros which are needed to model them. One reasonable interpretation is sketched in Fig. A 3.15. Next, try to find the corner frequencies at which the changes in slope occur (here 0.05 Hz and 5 Hz).

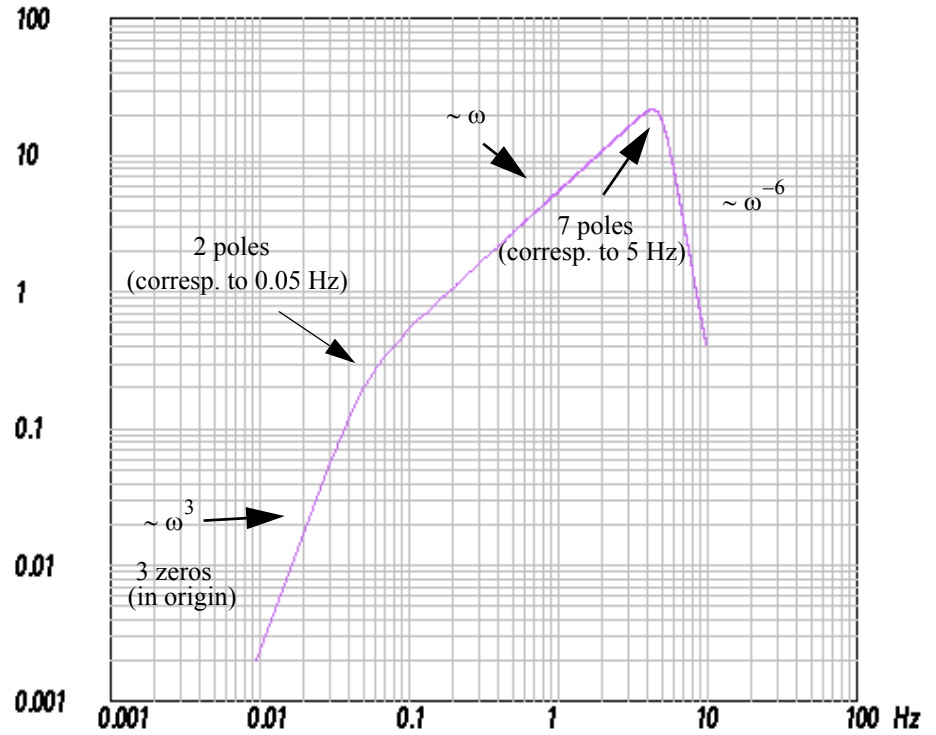


**Fig. A 3.15** Frequency response function (amplitude) with an 'unknown' pole - zero distribution from Problem 3.8.

Poles corresponding to the first corner frequency at 0.05 Hz have to be located either on the negative real axis of the s-plane at a distance of 0.31416 from the origin or occur in pairs defined by  $p_{1,2}^{0.5Hz} = -0.31416 \cdot (\cos \alpha \pm j \sin \alpha)$  with  $\alpha$  between 0 and  $90^\circ$ . If we choose  $45^\circ$  as a trial value, we obtain -0.2221 for the real part and  $\pm 0.2221$  for the imaginary part.

Poles corresponding to the second corner frequency at 5 Hz on the other hand have to be located either on the negative real axis at a distance of 31.416 from the origin or occur in pairs defined by  $p_{1,2}^{5Hz} = -31,416 \cdot (\cos\alpha \pm j\sin\alpha)$  with  $\alpha$  between 0 and  $90^\circ$ . If we put 1 pole on the negative real axis at (-31.416, 0) we are left with six poles to distribute as complex conjugate pairs. If we arbitrarily choose  $\alpha$  to be 25, 50, and  $75^\circ$ , we obtain the following pole positions:

(-0.2221, 0.2221)  
 (-0.2221, -0.2221)  
 (-28.473, 13.277)  
 (-28.473, -13.277)  
 (-20.194, 24.066)  
 (-20.194, -24.066)  
 (-8.131, 30.346)  
 (-8.131, -30.346)  
 (-31.416, 0)

This is displayed below (Fig. A 3.16).

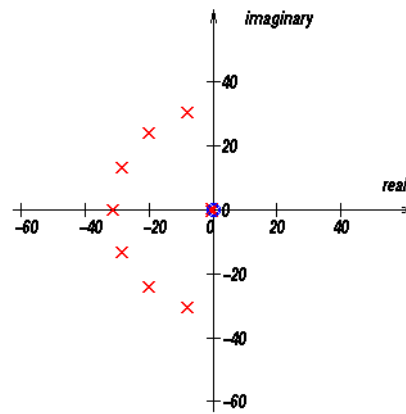


**Fig. A 3.16** Trial pole/zero position to match the amplitude frequency response function of Problem 3.8.

The corresponding amplitude frequency response function (not shown) matches the shape of the frequency response function shown in Fig. A 3.15 fairly well visually. The amplitude values, however, are too low by an approximate factor of  $2,5 \cdot 10^{10}$ . This can be adjusted by entering a scale factor of  $2.5e10$  in the *poles and zeros* input panel of DST.

Hint: For practical reasons regarding DST it is advisable to start out with the poles close to the origin and add the more distant poles only after the shape of the frequency response function has been matched in the low frequency range.

The resulting frequency response function now matches very closely the one given for Problem 3.8 (Fig. A 3.17).

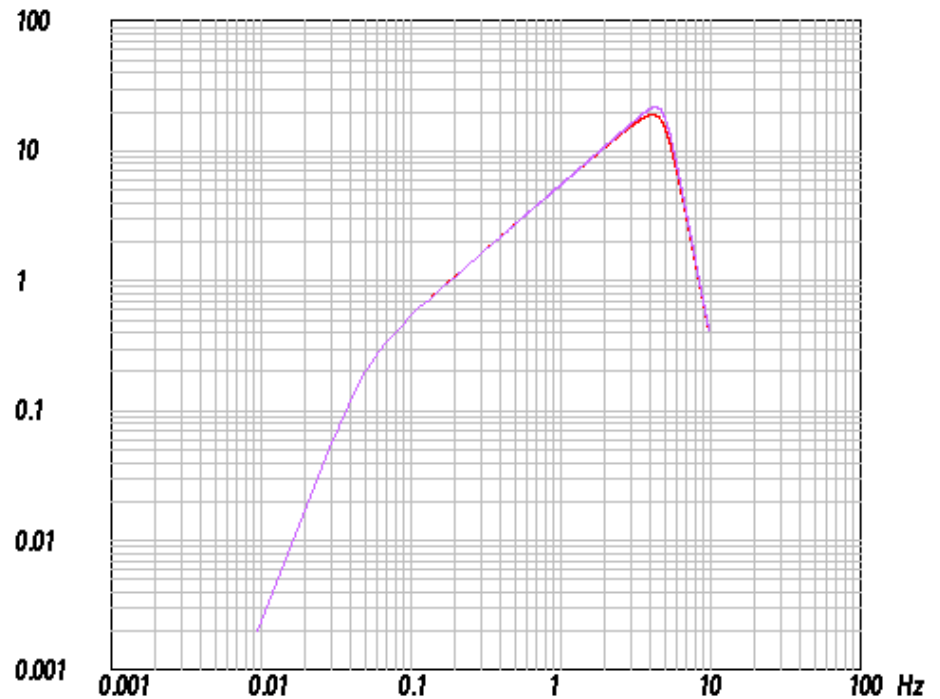


**Fig. A 3.17** Frequency response function of Problem 3.8 (upper curve) and frequency response function generated from the poles and zeros shown in Fig. A 3.16 with a scaling factor of  $2.5 \times 10$ .

At the corner frequency of 5 Hz, the frequency response function of Problem 3.8 has slightly higher amplitudes and shows a sharper change of slopes with respect to the trial frequency response function. This difference can be reduced by shifting some of the poles of the trial response closer to the imaginary axis to obtain a more "resonant" behaviour at that frequency.

The real distribution of poles and zeros for the frequency response function of Problem 3.8 is given below. It describes the frequency response function of the GRF array in SE Germany.

Poles:

(-0.2221, 0.2221)  
 (-0.2221, -0.2221)  
 (-7.0058, 30.6248)  
 (-7.0058, -30.6248)  
 (-19.5721, 24.5742)  
 (-19.5721, -24.5742)  
 (-28.3058, 13.6288)  
 (-28.3058, -13.6288)  
 (-31.4159, 0.0)

Zeros:

(0.0, 0.0)  
 (0.0, 0.0)  
 (0.0, 0.0)

Scale factor:

2.49059e10

For the generation of Fig. A 3.15 - Fig. A 3.17 within DST, an internal sampling frequency of 20 Hz and a window length of 2048 points was used.

## Chapter 4

*Solution 4.1* The time derivative of (4.26) is

$$\begin{aligned} \frac{dx_r(t)}{dt} = & -\varepsilon x_{r0} e^{-\varepsilon t} (c_1 \sin(\sqrt{\omega_0^2 - \varepsilon^2} t) + c_2 \cos(\sqrt{\omega_0^2 - \varepsilon^2} t)) \\ & + x_{r0} e^{-\varepsilon t} c_1 \sqrt{\omega_0^2 - \varepsilon^2} \cos(\sqrt{\omega_0^2 - \varepsilon^2} t) \\ & - x_{r0} e^{-\varepsilon t} c_2 \sqrt{\omega_0^2 - \varepsilon^2} \sin(\sqrt{\omega_0^2 - \varepsilon^2} t) \end{aligned} \quad (4.1-1)$$

With

$$c_3 = -(c_1 \varepsilon + c_2 \sqrt{\omega_0^2 - \varepsilon^2}) \quad (4.1-2)$$

and

$$c_4 = -(c_2 \varepsilon - c_1 \sqrt{\omega_0^2 - \varepsilon^2}) \quad (4.1-3)$$

we obtain

$$\frac{dx_r(t)}{dt} = x_{r0} e^{-\varepsilon t} (c_3 \sin(\sqrt{\omega_0^2 - \varepsilon^2} t) + c_4 \cos(\sqrt{\omega_0^2 - \varepsilon^2} t)) \quad (4.1-4)$$

As for the displacement seismometer, the amplitude ratio of two consecutive maxima or minima are solely determined by the exponential term. Therefore, equations (4.27) and (4.28) are valid for the determination of the damping constant of seismometers with velocity transducers as well.

*Solution 4.2* From Fig. 4.4 we can directly read the values of the first two consecutive peak amplitudes which are:  $a_1 = 0,0869349$ , the value of the maximum and  $a_2 = |-0,014175| = 0,014175$ , the value of the minimum of the calibration signal. Therefore, we obtain

$$\left( \frac{a_1}{a_2} = 6,13297 \right) \Rightarrow \frac{\Lambda}{2} = 1,81368 \quad (4.2-1)$$

From  $\Lambda = 3,6276$  we obtain  $h = 0.5$ . From Fig. 4.4 we measure the period from the second zero-crossing as  $T \approx 1,15$  sec (the exact value would be 1.15470054). This yields  $f_0 = 1\text{Hz}$ .

*Solution 4.3* The displacement impulse response is the inverse Fourier transform of:

$$T(j\omega) = \frac{\text{Output}(j\omega)}{\text{Input}_{\text{disp}}(j\omega)} \quad (4.3-1)$$

Now let us examine the input signal, a step function in acceleration, which is equivalent to the integral of a spike. Hence, by equivalence between integration in the time domain

and division by  $j\omega$  in the frequency domain, the frequency response of the input signal in acceleration is:

$$Input_{acc}(j\omega) = \frac{1}{j\omega} \cdot 1 \quad (4.3-2)$$

with 1 being the frequency response of an impulse (here in acceleration). In order to obtain the input signal in displacement, the input signal in acceleration has to be integrated twice. This corresponds to two times division by  $j\omega$ :

$$Input_{disp}(j\omega) = \left(\frac{1}{j\omega}\right)^2 \cdot Input_{acc}(j\omega) = \left(\frac{1}{j\omega}\right)^3 \quad (4.3-3)$$

Therefore,

$$T(j\omega) = \frac{Output_{disp}(j\omega)}{Input_{disp}(j\omega)} = 1 / \left(\frac{1}{j\omega}\right)^3 \quad (4.3-4)$$

which becomes

$$T(j\omega) = (j\omega)^3 \cdot Output_{vel}(j\omega) \quad (4.3-5)$$

In the time domain, multiplication with  $(j\omega)^3$  corresponds to triple differentiation. Since high frequency noise will be greatly enhanced by differentiation, this explains why this approach to obtaining the impulse response is often impractical.

**Solution 4.4** The pole positions for the three different damping factors are:

$$h = 0.25: -1.5708 \pm j 6.0837$$

$$h = 0.5: -3.14159 \pm j 5.4414$$

$$h = 0.62: -3.89557 \pm j 4.9298$$

The corresponding pole/zero maps, impulse responses and amplitude parts of the frequency response functions for these damping values are shown in Fig. A 4.1.

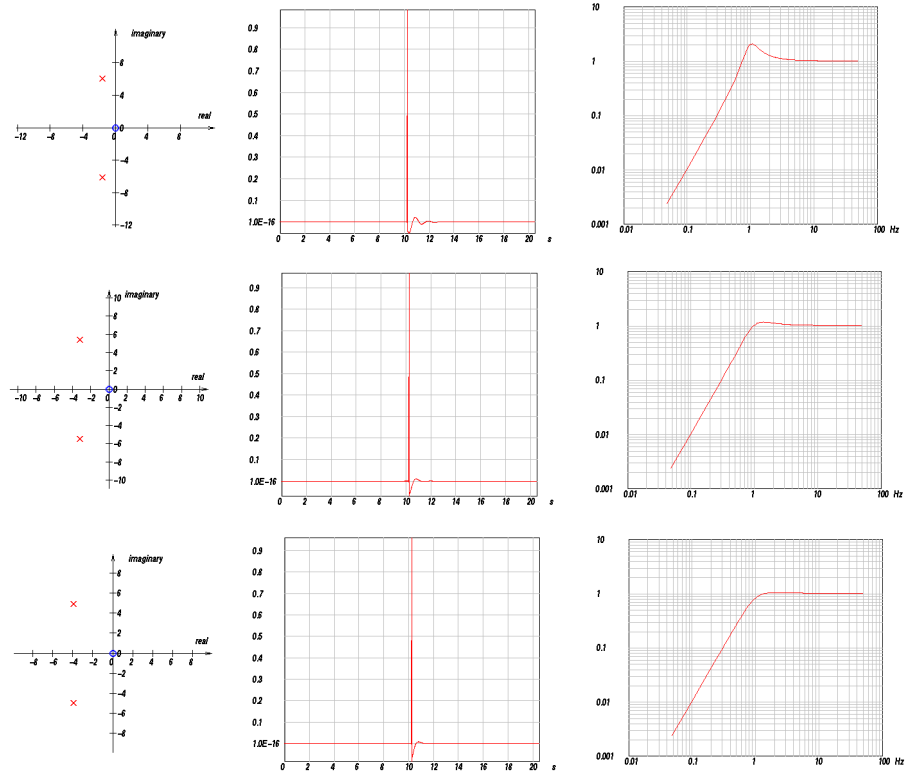


**Fig. A 4.1** Pole/zero maps (left column), impulse response functions (center column) and amplitude part of the frequency response functions (right columns) for a displacement seismometer with damping factors 0.25, 0.5, and 0.62 (from top to bottom). The internal sampling frequency in DST was set to 100 Hz (*Setup* menu).

You might notice some small precursory oscillations in the impulse response functions in Fig. A 4.1. The origin of this effect is discussed in detail in chapter 10.2.4.

*Solution 4.5* The output signal must be differentiated. This, however, corresponds to multiplication of the transfer function with  $s$ , a first degree polynomial with a single zero at the origin. Hence, in order to simulate the output of an electrodynamic system, simply add a zero at the origin to the transfer function. For the damping factor  $h = 0.62$ , the resulting amplitude frequency response is shown in Fig. A 4.2.

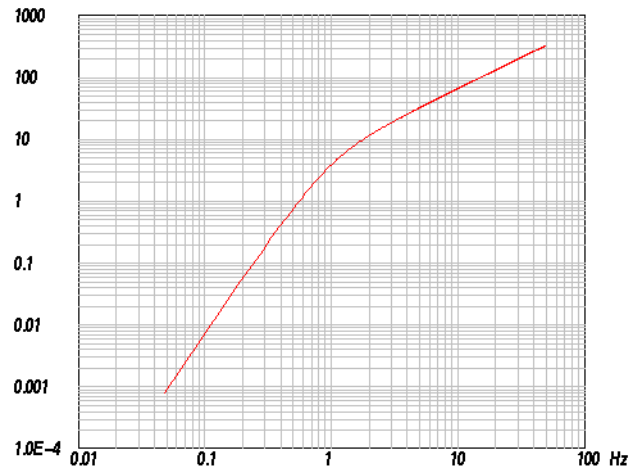


**Fig. A 4.2** Amplitude frequency response function for a 1 Hz velocity seismometer.

## Chapter 5

*Solution 5.1* First set the internal sampling frequency in DST to 1024 Hz and the window length to 2048 points (*Modify* option of the *Setup* menu). Next, generate the signals to be discretized using the *Sine/Cosine* option of the *Test Signals* menu. For the amplitude  $A$  and the phase  $PHI$  of the signal keep the value of 1 and 0, respectively. Start out with a signal frequency of 1 Hz and discretize and reconstruct this signal using a discretization frequency of 10 Hz. The result should agree with Fig. 5.2 - Fig. 5.4. The dominant frequency of the output signal can be easily obtained by measuring the dominant signal period on the DST screen in seconds and taking the reciprocal value. For the 1 Hz input signal the output signal frequency is 1 Hz also. Read the maximum signal amplitude of the output signal from the screen and enter input frequency, output frequency and maximum output amplitude into Table A 5.1.

**Table A 5.1** Corresponding input frequencies, output frequencies and output amplitudes for a discretization frequency of 10 Hz.

Signal frequency “input signal” [Hz]	Signal frequency “output signal” [Hz]	Signal amplitude (maximum) “output signal”
1	1	$\approx 1$
2		
3		
4		
5		
6		
7		
8		
9		
10		
11		
12		
13		
14		
15		
16		
17		
18		
19		
20		

Next, perform the same procedure with input signal frequencies from 2 - 20 Hz in steps of 1 Hz and fill in all entries in Table A 5.1.

For the interpretation imagine the "frequency band" as a band folded at  $1/2$  of the sampling frequency (folding frequency) and connect each input frequency with the corresponding output (alias-) frequency. As can be seen in Fig. A 5.1 the output frequencies can easily be obtained graphically by vertical projection from a particular input frequency on the "frequency band" down to the region between zero and the folding frequency.

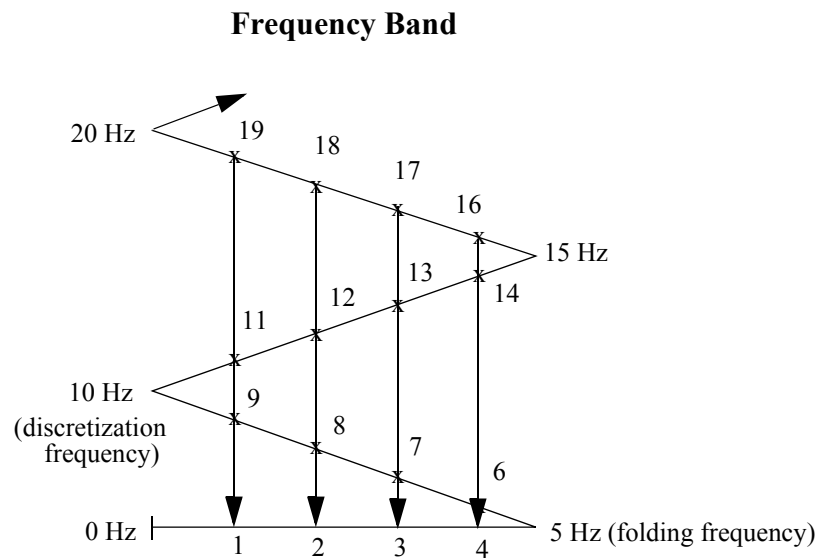


**Fig. A 5.1** Graphical illustration of the alias effect.

*Solution 5.2* For a discretization frequency of 10 Hz, the reconstruction breaks down for frequencies around 5 Hz. For exactly 5 Hz, it strongly depends on the value of the phase angle of the continuous signal, if the discretization results in non-zero values. For a phase angle of exactly zero, the signal is discretized exactly at the zero crossings. Hence it cannot be distinguished from a zero signal. Therefore, for a unique reconstruction the input signals have to be below  $1/2$  of 10 Hz ( $= 5$  Hz).

*Solution 5.3* The aliasing frequency corresponding to 18.5 Hz and a sampling frequency of 10 Hz would be 1.5 Hz (Fig. A 5.2).

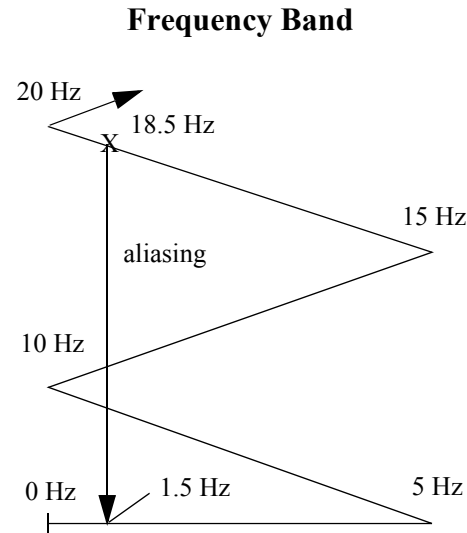


**Fig. A 5.2** Graphical determination of the alias frequency for a signal frequency of 18.5 Hz and a discretization frequency of 10 Hz..

## Chapter 6

*Solution 6.1* The Wood-Anderson magnitude is defined as  $M_{WA} = \log_{10}(A) - \log_{10}(A_0)$  with  $A$  the amplitude [in mm] measured on a Wood-Anderson displacement instrument and  $-\log_{10}(A_0)$  the distance correction which is exactly 3 for 100 km. The theoretical trace amplitude for a  $M_{WA} = 0$  earthquake on this instrument will be  $A_{M_{WA}=0} = 10^{0-3} = 0,001$  mm. For the magnitude 6 earthquake this value will be  $A_{M_{WA}=0} = 10^{6-3} = 1000$  mm. Hence the dynamic range needed is at least  $20 \cdot \log(10^6) = 120$  dB (20 bits).

*Solution 6.2* The maximum number we can express with 16 bit is  $2^{16} - 1$ . For a gain ranging ADC with 8 bit for the gain and 8 bit for the mantissa we can express the maximum number  $(2^8 - 1) \cdot 2^{(2^8 - 1)}$ . Therefore, with the particular gain ranging setting we

increase the dynamic range by the factor

$$\frac{(2^8 - 1) \cdot 2^{(2^8 - 1)}}{(2^{16} - 1)} = 2,25276 \cdot 10^{74}.$$

Expressed in the decibel scale, this would yield an improvement of 1487 dB. Notice that this is a fictitious improvement since on the other hand, the loss of 8 bit of resolution would be unacceptable in most practical applications.

*Solution 6.3* First, set the internal sampling frequency in DST to 100 Hz and the window length to 512 points (*Modify* option of the *Setup* menu). Next, generate the signal to be discretized using the *Spike(s)* option of the *Test Signals* menu. For the spike position enter a value of 256 to center the spike in the middle of the window. For the amplitude enter a value of 100. Subsequently integrate this signal (*Utilities* -> *Integration*) to produce a centered step function with a step amplitude of 1. Next, apply delta modulation (*Utilities*-> *Delta Modulation*) using a quantum value (LSB ) of 0.01 to obtain the following picture

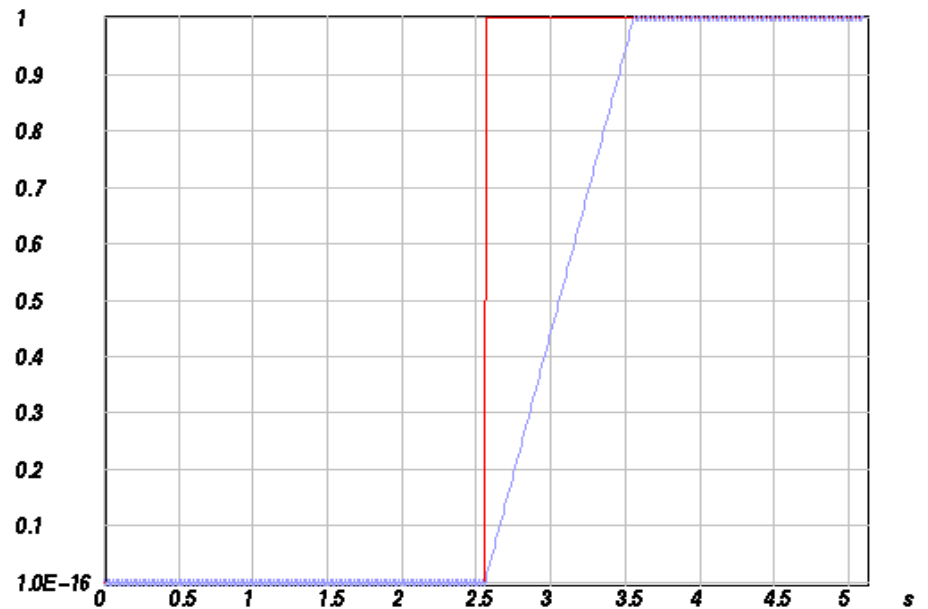


**Fig. A 6.1** Demonstration of slope overload and granular noise during delta modulation.

For the chosen parameters, the predicted input signal is unable to follow the rapid rise of the actual input signal. This effect is called *slope overload*. For the flat portions of the input signal, the predicted input signal oscillates around the actual input signal causing *granular noise*.

**Solution 6.4** In Fig. A 6.2 the performance of plain delta modulation is compared to delta modulation of the integrated signal omitting the integration in the demodulation part.

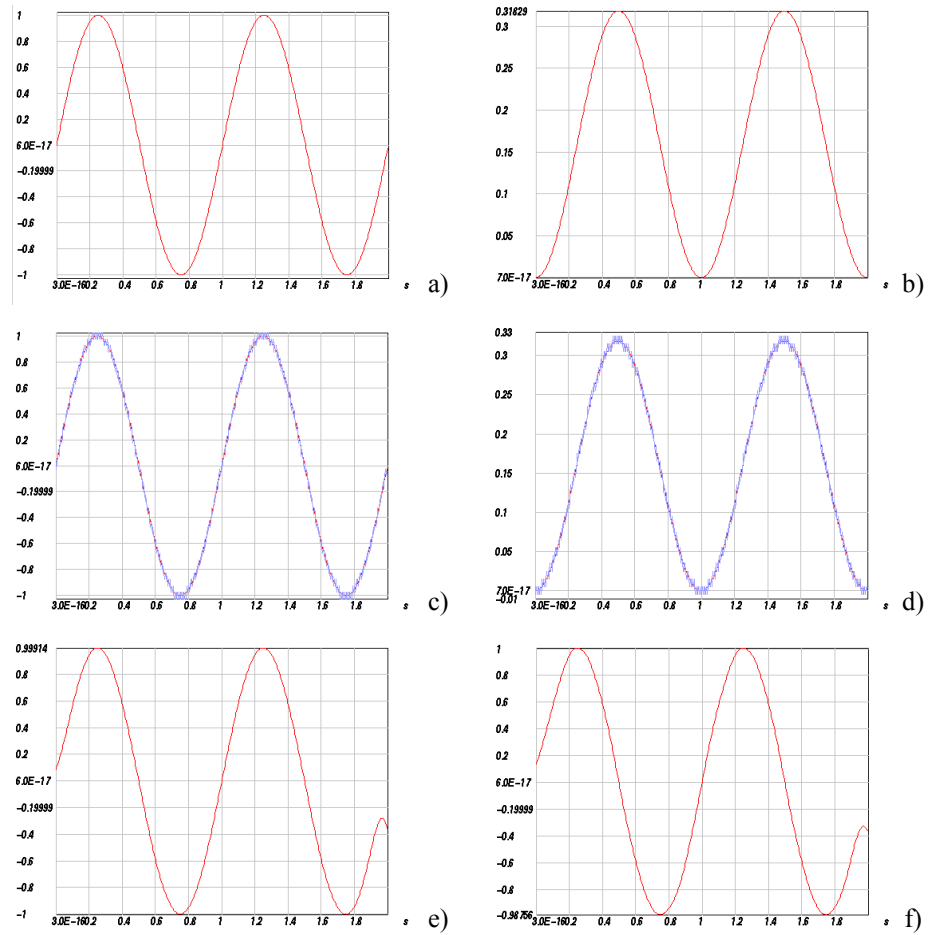


**Fig. A 6.2** Delta modulation and demodulation of a sinusoidal input signal with integration performed during demodulation (a, c, e) or before modulation (b, d, f).

The left panel in Fig. A 6.2 shows the sinusoidal input signal as defined in Problem 6.4 (a), the comparison of the actual input signal and predicted input signal (c), and the demodulated signal (e). The right hand panel shows in frame (b) the integrated sinusoid of Fig. A 6.2a), in frame (d) the comparison of the corresponding actual input signal and predicted input signal, and finally in frame (f) the low pass filtered modulator output signal. In the latter case the LSB value for the modulation of the integrated signal was reduced to 0.01 to account for the smaller maximum peak to peak amplitude. For the lowpass filter, in both cases a Butterworth filter with a corner frequency of 4 Hz and 1 section was chosen (*Utilities -> Butterworth Filter -> Lowpass*). As can be seen in Fig. A 6.2 the integration can be done either before modulation or before final lowpass filtering without changing the result. This could have been guessed already from the fact that integration is a linear operation.

**Solution 6.5** First set the internal sampling frequency in DST to 5120 Hz and the window length to 10240 points (*Modify* option of the *Setup* menu). Next, generate the 1 Hz sinusoidal signal to be discretized using the *Sine/Cosine* option of the *Test Signals* menu. For the amplitude  $A$  and the phase  $PHI$  of the signal take a value of 1 and 0, respectively. Use the *Sigma Delta Modulation* option from the *Utilities* menu of DST using a LSB of e. g. 1.2. The resulting trace will completely fill the screen. The final sampling frequency is generally reached in several stages. Here, use the *Decimation Filtering* option from the *Utilities* menu with a decimation ratio of 16 (resampling turned on) for the first stage. For the second stage use a decimation ratio of 4. Original sinusoid and resulting resampled trace are shown in Fig. A 6.3.

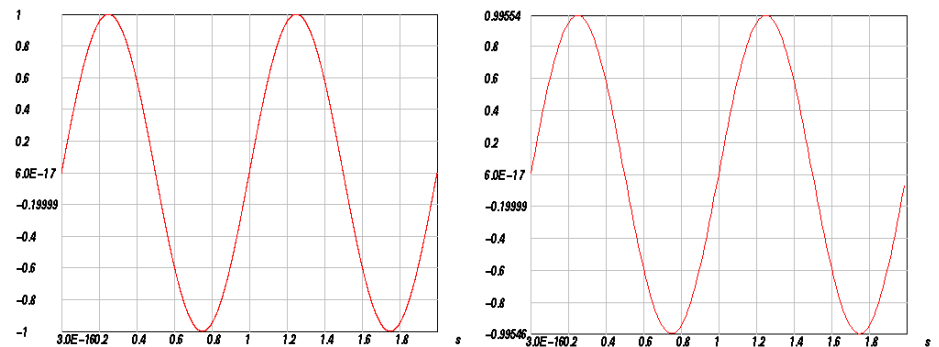


**Fig. A 6.3** Sigma-delta modulation simulation using DST. The left panel shows the input trace while the right panel displays the resulting resampled trace after sigma-delta modulation and two stages of decimation filtering.

## Chapter 7

*Solution 7.1* Since the signal is assumed to be zero outside the time window  $0 \leq t < NT$ , the Fourier transform becomes  $X(j\omega) = \int_0^{NT} x(t)e^{-j\omega t} dt$ . If we approximate the integral by a finite sum using the rectangular rule we obtain:

$$\int_0^{NT} x(t)e^{-j\omega t} dt \approx T \cdot \sum_{n=0}^{N-1} x[nT]e^{-j\omega nT} \quad (7.1-1)$$

For  $\omega = \omega_k = k \cdot \frac{2\pi}{TN}$  the right hand side becomes

$$\begin{aligned} T \cdot \sum_{n=0}^{N-1} x[nT]e^{-j\left(k \cdot \frac{2\pi}{TN}\right)nT} &= T \cdot \sum_{n=0}^{N-1} x[n]e^{-j\left(k \cdot \frac{2\pi}{N}\right)n} \\ &= T \cdot \tilde{X}[k] \end{aligned} \quad (7.1-2)$$

$\tilde{X}[k]$  is the DFT. Therefore,

$$X(j\omega)|_{\omega=\omega_k} = \int_0^{NT} x(t)e^{-j\omega_k t} dt \approx T \cdot \tilde{X}[k] \quad (7.1-3)$$

*Solution 7.2* Since the inverse Fourier transform evaluates the inverse z-transform on the unit circle, this means that the banded convergence region is chosen. Hence, it will correspond to a two-sided impulse response.

*Solution 7.3* a) positive time shifts  $n_0$  will cause a multiplication of the z-transform with a term  $z^{-n_0}$  which has a pole of order  $n_0$  at the origin ( $1/0^{n_0}$ ). b) negative time shifts  $n_0$  will cause a multiplication of the z-transform with a term  $z^{n_0}$  which has a pole at infinity. Hence, depending on the sign of the shift, time shifts add poles at either the origin or at infinity of the z-plane.

*Solution 7.4* Let's assume we have two sequences with 1024 samples and a spike at position 1024 in each of them. If we convolve the two sequences in the time domain we expect the result to be a spike at position 2047. Hence, we have to pad up to this sample. If we have two sequences of different length, we have to pad both sequences up to one point less than twice the length of the longer sequence.

## Chapter 8

*Solution 8.1* In order to see how roots on the unit circle affect the properties of the impulse response of FIR filters, we first consider an impulse response function of length  $M + 1 = 3$ . Its z-transform in the notation of (8.18) corresponds to a simple quadratic

$q + pz + z^2$  with the two roots  $z_{1,2} = -\frac{p}{2} \pm \sqrt{\frac{p^2}{4} - q} = re^{\pm j\Phi}$  for which the following two properties hold:  $z_1 + z_2 = -p$  and  $z_1 \cdot z_2 = q$ .

Since the wavelet is defined by the triplet  $(q, p, 1)$ , we need to determine  $q$  and  $p$ . For complex conjugate roots  $re^{\pm j\Phi}$  it follows that  $q = z_1 \cdot z_2 = re^{j\Phi} \cdot re^{-j\Phi} = r^2$ . Using Euler's formulas, we deduce that  $-p = z_1 + z_2 = re^{j\Phi} + re^{-j\Phi} = 2r\cos\Phi$ . Hence, the discrete finite impulse response for a system with the two complex conjugate roots  $re^{\pm j\Phi}$  will consist of the triplet

$$(q, p, 1) = (r^2, -2r\cos\Phi, 1) \quad (8.1-1)$$

If the roots are on the unit circle ( $r = 1$ ), the result will be a *symmetric impulse response*. This will also be the case for higher order systems which only contain zeros on the unit circle since the convolution of symmetric impulse response functions remains symmetric. Because of this symmetry, one could think that in the context of removing all noncausal effects roots on the unit circle can be corrected for. However, this is not the case since a system with only roots on the unit circle has only a single waveform representation for the given amplitude spectrum. To see this we again consider an arbitrary

second order system  $A_1(z)$  with the two complex conjugate roots  $z_{1,2} = r_1 e^{\pm j\Phi_1}$ .

Replacing the poles or zeros of a transfer function by their complex conjugate reciprocals does not change the 'amplitude spectrum' of the signal except for a constant scaling factor as we have already seen before. Therefore, the system  $A_2(z) = A_1(1/z)$  with

the roots  $z_{3,4} = 1/r_1 \cdot e^{\mp j\phi_1}$  has the same amplitude spectrum as  $A_1(z)$ . In the general case in which the roots are assumed to be located away from the unit circle ( $r_1 \neq 1, r_2 \neq 1$ ) the waveforms of  $A_1(z)$  and  $A_2(z)$  will be different (cf. (8.1-1)). They are obtained by setting  $r$  and  $\phi$  in (8.1-1) to  $r_1$  and  $\phi_1$  and to  $1/r_1$  and  $-\phi_1$  for the first and the second representation, respectively. These are the only two waveform representations for the amplitude spectrum of  $A_1(z)$ . One could naively argue that replacing only a single root by its reciprocal would not affect the amplitude spectrum as well. However, the roots of any real sequence of a second order system must always occur as a pair of complex conjugate roots, which would be violated in this case.

For higher order systems the number of wavelets with the same amplitude spectrum increases but this is irrelevant in the context of the present argument. Now we consider a second order system in which the roots are located directly on the unit circle. In this case, because  $r_1 = 1$  the root pairs of  $A_1(z)$  and  $A_2(z)$  become identical

$z_{1,2} = z_{3,4} = e^{\pm j\Phi}$ . Consequently, the system has only a single waveform representation. The same argument can be made for higher order systems.

In the context of removing the acausal FIR filter response we can therefore ignore the contribution of roots on the unit circle (UC roots) because the corresponding waveform component will not be changed by the correction filter process. In effect, this is equivalent to treating the roots on the unit circle as belonging to the minimum phase component.

*Solution 8.2* Load the data trace `example20HZ` into DST using the *File -> Open File with Data Trace* option from the main menu. The file is found in subdirectory `FIR20HZ`. Next, use option *Interpolate* in the *Utilities* menu with an interpolation factor of 2 to obtain an interpolated trace sampled at 40 Hz. Subsequently use option *FIR2CAUS* in the *Utilities* menu with the correction filter file `quant40Hz.prt`. If you choose 0 for the number of zeros to pre/append/ to the filtered trace and select correction for linear phase, the resulting "corrected" trace is shown in Fig. A 8.1. Option *Ok* directly results in the corrected trace. If you choose *Apply* for the *FIR2CAUS* option, you will see both the uncorrected and the corrected trace displayed together. Using the left mouse button, you can zoom in on the P-wave onset as shown in Fig. A 8.1.

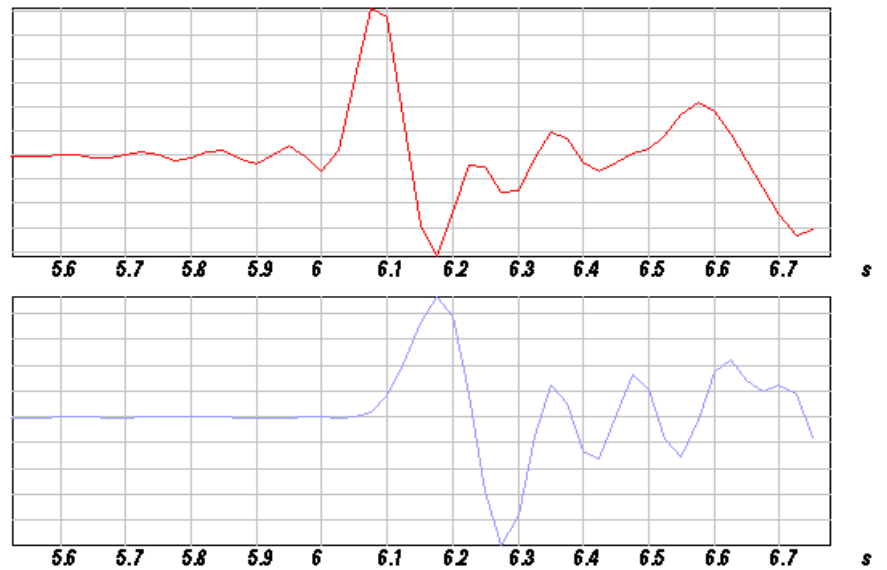


**Fig. A 8.1** Removing the maximum phase component of the FIR filter response from the example data trace `example20HZ`. The top trace shows the P- wave onset of the uncorrected trace while the bottom trace shows the corrected signal.

## Chapter 9

*Solution 9.1* In order to comply with the sampling theorem, digital recording systems must have an anti-alias filter for which the transfer function has to have zeros at the Nyquist frequency. Therefore, in addition to the irregularity at zero frequency discussed in the text, an irregularity problem will show up at the Nyquist frequency.

*Solution 9.2* Since a minimum phase system  $T_{act}^{min}(z)$  has all its poles and zeros inside of the unit circle, this is true also for the inverse system  $1/T_{act}^{min}(z)$ . The poles of  $T_{act}^{min}(z)$  have become zeros in  $1/T_{act}^{min}(z)$  and vice versa. Hence, the inverse of a minimum phase system is always minimum phase as well. Since minimum phase systems are always stable (all poles are inside the unit circle since all singularities are inside the unit circle), **minimum phase systems always have stable causal inverse systems.**

$T_{act}^{max}(z)$  on the other hand as a maximum phase system has all its zeros outside the unit circle. These will become poles in  $1/T_{act}^{max}(z)$  and as a consequence  $1/T_{act}^{max}(z)$  will not have a stable causal impulse response.

*Solution 9.3* The continuous transfer function of the displacement seismometer is

$$T(s) = \frac{s^2}{s^2 + 2h_1\omega'_{01}s + \omega_{01}^2} \quad (9.3-1)$$

With frequency warping this becomes

$$T(s) = \frac{s^2}{s^2 + 2h_1\omega'_{01}s + \omega_{01}^2} \quad (9.3-2)$$

Replacing  $s$  by  $(2/T) \cdot (1 - z^{-1})/(1 + z^{-1})$  and  $\omega'_{01}$  by  $(2/T) \cdot \tan(\omega_{01}T/2)$  we obtain

$$T_{sim}(z) = \frac{\left(\frac{1 - z^{-1}}{1 + z^{-1}}\right)^2}{\left(\frac{1 - z^{-1}}{1 + z^{-1}}\right)^2 + 2h_1 \tan\left(\omega_{01}\frac{T}{2}\right)\left(\frac{1 - z^{-1}}{1 + z^{-1}}\right) + \tan^2\left(\omega_{01}\frac{T}{2}\right)} \quad (9.3-3)$$

Multiplying numerator and denominator by  $(1 + z^{-1})^2$  yields

$$T_{sim}(z) = \frac{(1 - z^{-1})^2}{(1 - z^{-1})^2 + 2h_1 \tan\left(\omega_{01}\frac{T}{2}\right)(1 - z^{-1})(1 + z^{-1}) + \tan^2\left(\omega_{01}\frac{T}{2}\right)(1 + z^{-1})^2} \quad (9.3-4)$$

The numerator polynomial is simply  $1 - 2z^{-1} + z^{-2}$ , hence we get  $b_0 = 1$ ,  $b_1 = -2$ , and  $b_2 = 1$ . We obtain the denominator polynomial by expanding the denominator in powers of  $z^{-1}$  which becomes

$$\begin{aligned}
& 1 - 2z^{-1} + z^{-2} + 2h_1 \tan(\omega_{01} T/2) - 2h_1 \tan(\omega_{01} T/2) z^{-2} \\
& + \tan^2(\omega_{01} T/2) + 2 \tan^2(\omega_{01} T/2) z^{-1} + \tan^2(\omega_{01} T/2) z^{-2} \\
& = \\
& 1 + 2h_1 \tan(\omega_{01} T/2) + \tan^2(\omega_{01} T/2) \\
& + (-2 + 2 \tan^2(\omega_{01} T/2)) \cdot z^{-1} \\
& + (1 - 2h_1 \tan(\omega_{01} T/2) + \tan^2(\omega_{01} T/2)) \cdot z^{-2}
\end{aligned} \tag{9.3-5}$$

Hence we obtain

$$\begin{aligned}
a_0 &= 1 + 2h_1 \tan(\omega_{01} T/2) + \tan^2(\omega_{01} T/2) \\
a_1 &= -2 + 2 \tan^2(\omega_{01} T/2) \\
a_2 &= 1 - 2h_1 \tan(\omega_{01} T/2) + \tan^2(\omega_{01} T/2)
\end{aligned} \tag{9.3-6}$$

For  $\omega_{01} = 2\pi \cdot 0,008333[\text{Hz}] = 0,052358$ ,  $h_1 = 0,707$ , and  $T = 0,05[\text{s}]$  we finally get

$$\begin{aligned}
a_0 &= 1,00185 \\
a_1 &= -2,0 \\
a_2 &= 0,998151
\end{aligned} \tag{9.3-7}$$

The performance of the filter is demonstrated in Fig. A 9.1.

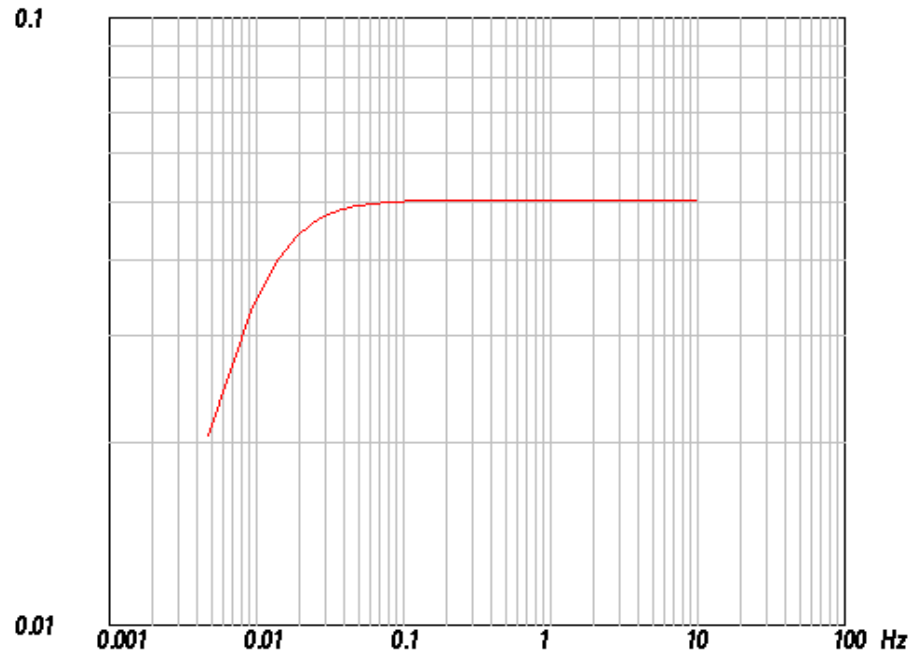


**Fig. A 9.1** Modulus of the frequency response function of a hypothetical seismometer with  $h = 0,707$  and  $\omega = 0,052358$ .

Fig. A 9.1 was created within DST evaluating the filter output signal  $y[i]$  from the filter input signal  $x[i]$  and the AR coefficients  $a[k]$  for  $k = 0 - N$  and  $b[l]$  for  $l = 0 - M$  using following difference equation

$$y[i] = \sum_{k=1}^N -\left(\frac{a[k]}{a[0]}\right) \cdot y[i-k] + \sum_{l=0}^M \frac{b[l]}{a[0]} \cdot x[i-l] \quad (9.3-8)$$

First, the internal sampling frequency and the window length were set to 20 Hz and 4096 points, respectively. Next, a spike test signal was created at position 100 with an amplitude of 1 using the *Test Signals -> Spike(s)* option of DST. The resulting trace was filtered using the *Utilities -> Difference Equation* option in DST with autoregressive coefficients 1.00185, -2.0, 0.998151 and moving average coefficients 1, -2, 1. The gain factor was left at 1.0 and the *Filtering inverse option* was left off. Finally, Fig. A 9.1 was obtained using the *Utilities -> Spectrum -> Amplitude -> log-log* option of DST.

*Solution 9.4* The continuous transfer function of the inverse filter is

$$T^{-1}(s) = \frac{s^2 + 2h_1\omega_{01}s + \omega_{01}^2}{s^2} \quad (9.4-1)$$

With the frequency warping this becomes

$$T^{-1}(s) = \frac{s^2 + 2h_1\omega'_{01}s + \omega_{01}^2}{s^2} \quad (9.4-2)$$

Replacing  $s$  by  $(2/T) \cdot (1 - z^{-1})/(1 + z^{-1})$  and  $\omega'_{01}$  by  $(2/T) \cdot \tan(\omega_{01}T/2)$  we obtain

$$T_{sim}(z) = \frac{\left(\frac{1 - z^{-1}}{1 + z^{-1}}\right)^2 + 2h_1 \tan(\omega_{01}T/2) \left(\frac{1 - z^{-1}}{1 + z^{-1}}\right) + \tan^2(\omega_{01}T/2)}{\left(\frac{1 - z^{-1}}{1 + z^{-1}}\right)^2} \quad (9.4-3)$$

Multiplying numerator and denominator by  $(1 + z^{-1})^2$  yields

$$T_{sim}(z) = \frac{(1 - z^{-1})^2 + 2h_1 \tan(\omega_{01}T/2)(1 - z^{-1})(1 + z^{-1})}{(1 - z^{-1})^2} + \frac{\tan^2(\omega_{01}T/2)(1 + z^{-1})^2}{(1 - z^{-1})^2} \quad (9.4-4)$$

The common denominator polynomial is simply  $1 - 2z^{-1} + z^{-2}$ , hence we get  $a_0 = 1$ ,  $a_1 = -2$ , and  $a_2 = 1$ . We obtain the numerator polynomial by expanding the numerator in powers of  $z^{-1}$  which becomes

$$\begin{aligned}
& 1 - 2z^{-1} + z^{-2} + 2h_1 \tan(\omega_{01} T/2) - 2h_1 \tan(\omega_{01} T/2) z^{-2} \\
& + \tan^2(\omega_{01} T/2) + 2 \tan^2(\omega_{01} T/2) z^{-1} + \tan^2(\omega_{01} T/2) z^{-2} \\
& = \\
& 1 + 2h_1 \tan(\omega_{01} T/2) + \tan^2(\omega_{01} T/2) \\
& + (-2 + 2 \tan^2(\omega_{01} T/2)) \cdot z^{-1} \\
& + (1 - 2h_1 \tan(\omega_{01} T/2) + \tan^2(\omega_{01} T/2)) \cdot z^{-2}
\end{aligned} \tag{9.4-5}$$

Hence we obtain

$$\begin{aligned}
b_0 &= 1 + 2h_1 \tan(\omega_{01} T/2) + \tan^2(\omega_{01} T/2) \\
b_1 &= -2 + 2 \tan^2(\omega_{01} T/2) \\
b_2 &= 1 - 2h_1 \tan(\omega_{01} T/2) + \tan^2(\omega_{01} T/2)
\end{aligned} \tag{9.4-6}$$

For  $\omega_{01} = 2\pi \cdot 0,00833[\text{Hz}] = 0,052358$  ,  $h_1 = 0,707$  , and  $T = 0,05[\text{s}]$  we finally get

$$\begin{aligned}
b_0 &= 1,00185 \\
b_1 &= -2,0 \\
b_2 &= 0,998151
\end{aligned} \tag{9.4-7}$$

The performance of the filter is demonstrated in Fig. A 9.2.

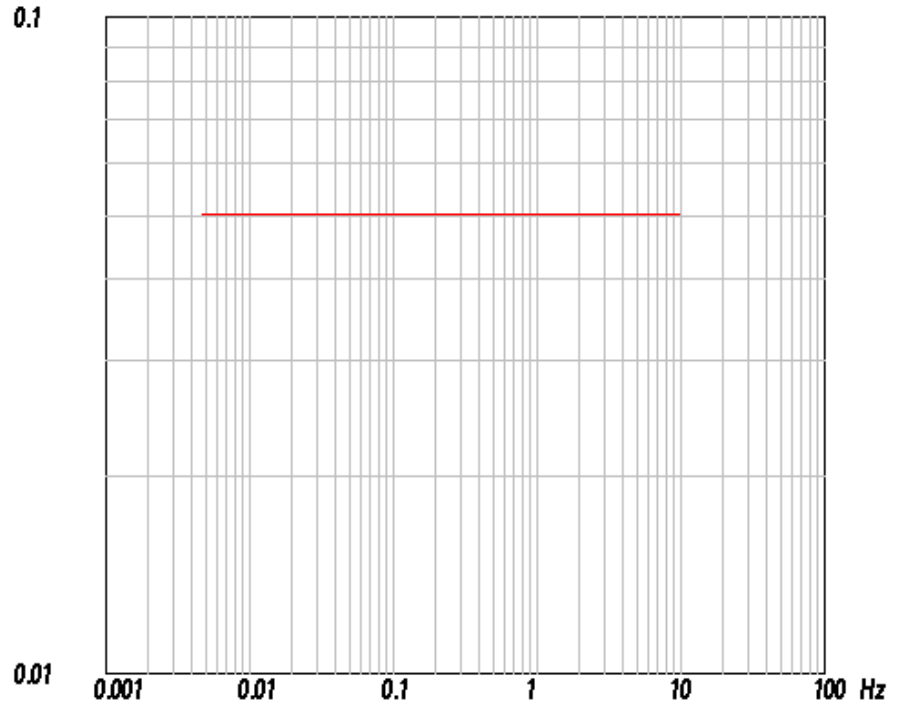


**Fig. A 9.2** Result of applying a deconvolution filter to the hypothetical seismometer response with  $h = 0,707$  and  $\omega = 0,052358$  shown in Fig. A 9.1. Displayed is the modulus of the resulting frequency response. The fact that the resulting frequency response is flat demonstrates the good performance of the deconvolution filter.

*Solution 9.5* In this case, the continuous transfer function of inverse filter is

$$T^{-1}(s) = \frac{s^2 + 2h_1\omega_{01}s + \omega_{01}^2}{s^3} \quad (9.5-1)$$

With the frequency warping this becomes

$$T^{-1}(s) = \frac{s^2 + 2h_1\omega'_{01}s + \omega'^2_{01}}{s^3} \quad (9.5-2)$$

Replacing  $s$  by  $(2/T) \cdot (1 - z^{-1})/(1 + z^{-1})$  and  $\omega'_{01}$  by  $(2/T) \cdot \tan(\omega_{01}T/2)$  we

obtain

$$T_{sim}(z) = \frac{T}{2} \cdot \frac{\left(\frac{1-z^{-1}}{1+z^{-1}}\right)^2 + 2h_1 \tan\left(\omega_{01} \frac{T}{2}\right) \left(\frac{1-z^{-1}}{1+z^{-1}}\right) + \tan^2\left(\omega_{01} \frac{T}{2}\right)}{\left(\frac{1-z^{-1}}{1+z^{-1}}\right)^3} \quad (9.5-3)$$

Multiplying numerator and denominator by  $(1+z^{-1})^3$  yields

$$\begin{aligned} T_{sim}(z) = & \frac{(1-z^{-1})^2 \cdot (1+z^{-1})}{(1-z^{-1})^3} \cdot \frac{T}{2} \\ & + \frac{2h_1 \tan(\omega_{01} T/2) (1-z^{-1})(1+z^{-1})^2}{(1-z^{-1})^3} \cdot \frac{T}{2} \\ & + \frac{\tan^2(\omega_{01} T/2) (1+z^{-1})^3}{(1-z^{-1})^3} \cdot \frac{T}{2} \end{aligned} \quad (9.5-4)$$

The common denominator polynomial is simply  $1 - 3z^{-1} + 3z^{-2} - z^{-3}$ , hence we get  $a_0 = 1$ ,  $a_1 = -3$ ,  $a_2 = 3$  and  $a_3 = -1$ . We obtain the numerator polynomial by expanding the numerator in powers of  $z^{-1}$  which becomes

$$\begin{aligned}
& (T/2)\{1 - z^{-1} - z^{-2} + z^{-3} \\
& + 2h_1 \tan\left(\omega_{01}\frac{T}{2}\right) + 2h_1 \tan\left(\omega_{01}\frac{T}{2}\right)z^{-1} - 2h_1 \tan\left(\omega_{01}\frac{T}{2}\right)z^{-2} - 2h_1 \tan\left(\omega_{01}\frac{T}{2}\right)z^{-3} \\
& + \tan^2\left(\omega_{01}\frac{T}{2}\right) + 3 \tan^2\left(\omega_{01}\frac{T}{2}\right)z^{-1} + 3 \tan\left(\omega_{01}\frac{T}{2}\right)^2 z^{-2} + \tan^2\left(\omega_{01}\frac{T}{2}\right)z^{-3}\} \\
& = \\
& (T/2)\{1 + 2h_1 \tan\left(\omega_{01}\frac{T}{2}\right) + \tan^2\left(\omega_{01}\frac{T}{2}\right) \\
& + \left(-1 + 2h_1 \tan\left(\omega_{01}\frac{T}{2}\right) + 3 \tan^2\left(\omega_{01}\frac{T}{2}\right)\right) \cdot z^{-1} \\
& + \left(-1 - 2h_1 \tan\left(\omega_{01}\frac{T}{2}\right) + 3 \tan^2\left(\omega_{01}\frac{T}{2}\right)\right) \cdot z^{-2} \\
& + \left(1 - 2h_1 \tan\left(\omega_{01}\frac{T}{2}\right) + \tan^2\left(\omega_{01}\frac{T}{2}\right)\right) \cdot z^{-3}\}
\end{aligned} \tag{9.5-5}$$

Hence we obtain

$$\begin{aligned}
b_0 &= T/2 + Th_1 \tan\left(\omega_{01}\frac{T}{2}\right) + (T/2)\tan^2\left(\omega_{01}\frac{T}{2}\right) \\
b_1 &= -T/2 + Th_1 \tan\left(\omega_{01}\frac{T}{2}\right) + (1,5T)\tan^2\left(\omega_{01}\frac{T}{2}\right) \\
b_2 &= -T/2 - Th_1 \tan\left(\omega_{01}\frac{T}{2}\right) + (1,5T)\tan^2\left(\omega_{01}\frac{T}{2}\right) \\
b_3 &= (T/2) - Th_1 \tan\left(\omega_{01}\frac{T}{2}\right) + (T/2)\tan^2\left(\omega_{01}\frac{T}{2}\right)
\end{aligned} \tag{9.5-6}$$

For  $\omega_{01} = 2\pi \cdot 0,00833[Hz] = 0,052358$  ,  $h_1 = 0,707$  , and  $T = 0,05[s]$  we finally get

$$\begin{aligned}
b_0 &= 0,0250463 \\
b_1 &= -0,0249536 \\
b_2 &= -0,0250461 \\
b_3 &= 0,0249538
\end{aligned} \tag{9.5-7}$$

The performance of the filter is demonstrated in Fig. A 9.3 with the P wave window of the vertical component record of the deep Bolivia earthquake of 94/06/09 recorded at station FUR of the German Regional Seismic Network. The data file FUR\_940609.20HZ.Z is found in subdirectory FUR using the *File -> Open File with Data Trace* option from the main menu of DST. Here only the P wave onset is displayed.

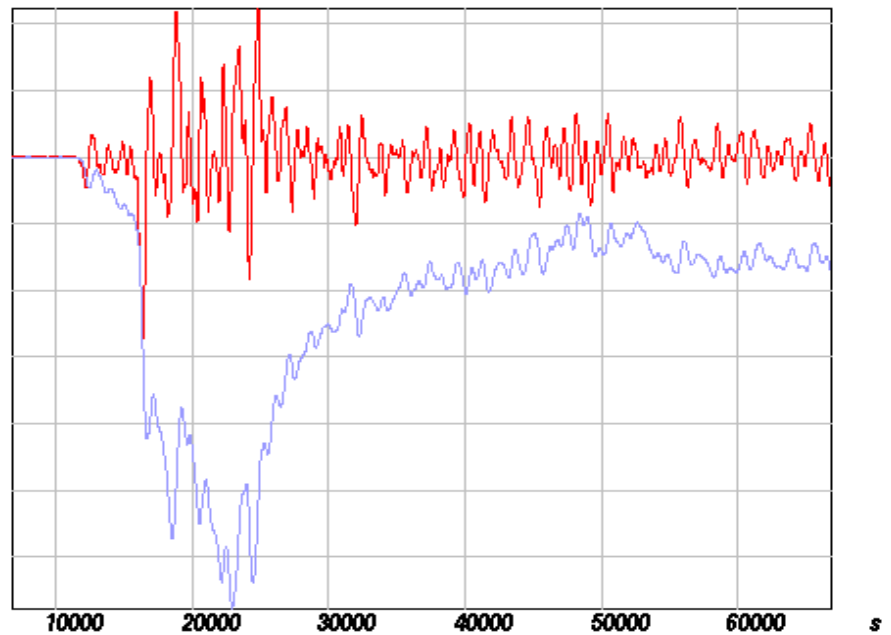


**Fig. A 9.3** P wave window of the vertical component record of the deep Bolivia earthquake of 94/06/09 recorded at station FUR of the German Regional Seismic Network. The top trace shows the BB 'velocity' record while the bottom trace shows the result of applying the deconvolution filter.

## Chapter 10

*Solution 10.1* These signals can be reproduced within DST by producing a spike test signal for an internal sampling frequency of 20 Hz and a trace length of 256 points and a spike of amplitude 1 at position 10. Trace 1 was produced by causal bandpass filtering the spike trace with a Butterworth bandpass consisting of 3 sections (6 poles) and corner frequencies at 0.4 and 1.5 Hz. Trace 2 corresponds to the spike trace filtered by a 6 pole Butterworth lowpass filter with a cut off frequency of 1.5 Hz. Trace 3 finally consists of a sinusoidal signal of 1 Hz signal frequency, amplitude of 1, and zero phase, again for 20

Hz sampling frequency and a trace length of 1024 points.

The frequency response function is defined by the following 9 poles:

```
-0.20762  0
-0.71256  1.03508
-0.71256 -1.03508
  -7.18   +17.42
  -7.18   -17.42
 -17.42   +7.18
 -17.42   -7.18
 -37.04   0
 -45.45   0
```

and 4 zeros at the origin. The corresponding GSE calibration file can be loaded into DST using the *File -> Open File With GSE Calibration* option from the main menu (file: `pr10_1.cal`). Looking at the amplitude frequency response function in Fig. A 10.1, we notice approximately three regions with different slope in the log-log plot. Outside of the central frequency band, roughly below 0.2 and above 2.5 Hz, the amplitude frequency response function decays rapidly, hence signals with frequencies outside this range are strongly attenuated while signals with frequencies between 0.2 and 2.5 Hz could be well recorded. With what we have learned about seismometer systems, we could expect that the frequencies of 0.2 and 2.5 Hz correspond to the eigenfrequency of the seismometer and the corner frequency of the anti-alias filter, respectively. This frequency band is commonly defined as the passband of the instrument. Within the passband, we see that the amplitude frequency response function is proportional to  $\omega$  so from the correspondence between multiplication by  $j\omega$  in the frequency domain and differentiation in the time domain we could expect that the frequency response function is that of an electrodynamic system. In this case, all signals falling completely within the passband would be expected to be differentiated. By comparing the spectra in Fig. 10.4 and the frequency response function in Fig. 10.5, we would expect this to happen for traces 1 and 3.

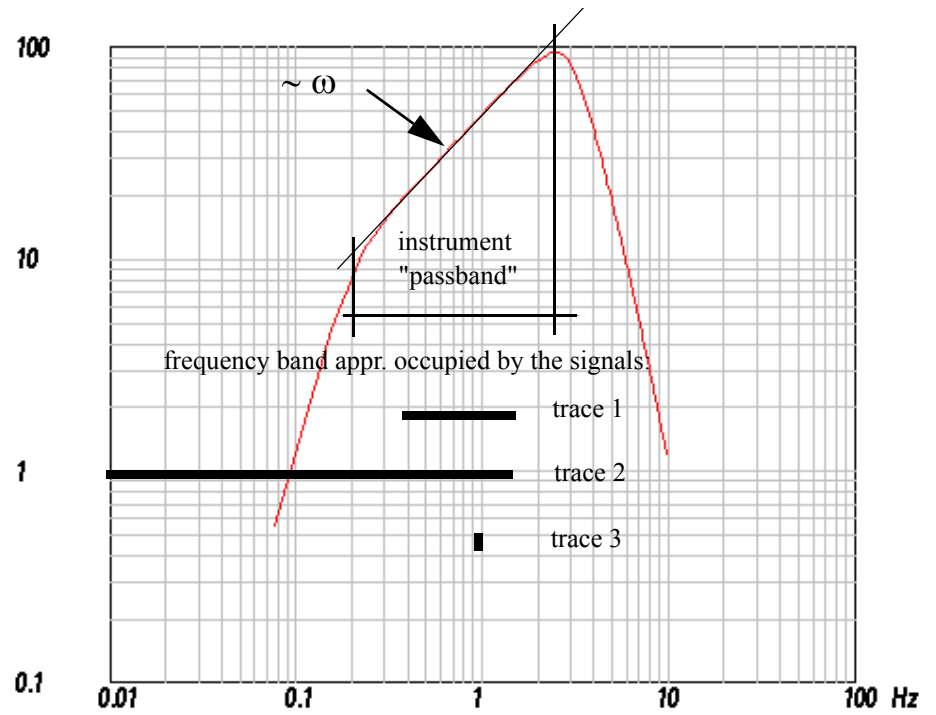


**Fig. A 10.1** Amplitude frequency response function for Problem 10.1.

The actual result for trace 1 is shown in Fig. A 10.2. The waveform of the filtered output signal is essentially identical to the scaled and differentiated input signals. Slight differences can be understood from the fact that the signal contains small amounts of energy outside the passband.

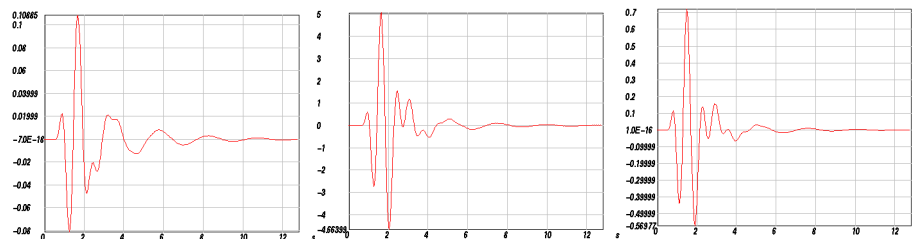


**Fig. A 10.2** The traces from left to right show the input signal trace 1 from Fig. 10.3, the output signal from filtering with the system displayed in Fig. A 10.1, and the differentiated input signal.

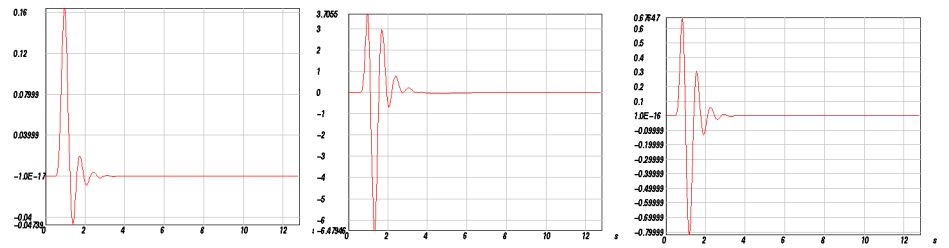


**Fig. A 10.3** The traces from left to right show the input signal trace 2 from Fig. 10.3, the output signal from filtering with the system displayed in Fig. A 10.1, and the differentiated input signal.

For trace 2 (Fig. A 10.3), the differences between the filtered trace and the differentiated trace are stronger since the input signal contains considerable amounts of energy outside the passband of the instrument (Fig. A 10.1).

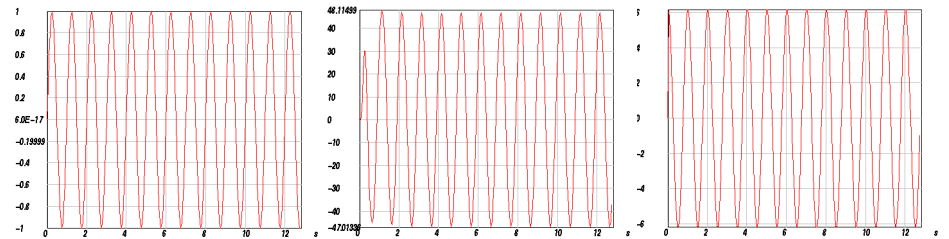


**Fig. A 10.4** The traces from left to right show the input signal trace 3 from Fig. 10.3, the output signal from filtering with the system displayed in Fig. A 10.1, and the differentiated input signal.

In Fig. A 10.4 it is shown how the fictitious instrument acts on a sinusoidal signal with 1.0 Hz signal frequency. What we can observe nicely is that the output signal is again a sinusoid with the same frequency. This is an important result which relates to the eigenvector property of the harmonic functions for LTI systems. Only amplitude and phase are changed. However, we can also see that there is a phase shift between trace 2 and 3. Hence, for the monochromatic signal with a signal frequency completely within the region of the frequency response function where its modulus is proportional to  $\omega$ , the output signal is not simply the differentiated signal which would show a phase shift to the input signal of  $90^\circ$ . If we calculate the phase shift for the given signal frequency of 1 Hz from the pole and zero distribution using the techniques learned earlier, we obtain approximately  $37^\circ$  which clearly differs from  $90^\circ$  which we would expect for pure differentiation.

How does this fit in with the fact that for the signal in Fig. A 10.4 the difference between the signal filtered with the instrument does not differ significantly from the differentiated

signal? The answer lies in the linear phase components of the frequency response function. Linear phase components do not cause any signal distortion but only a time shift of the output signal. With other words, we could also explain the phase shift seen for the monochromatic signal as being produced by a time shift and a differentiation. However, in order to test this hypothesis we would have to analyse the properties of the phase of the frequency response function in more detail. In this context, however, I only want to remind you that the circumstances under which it is justified to speak of a *displacement*- or a *velocity system* depend on a number of factors and that we should be careful not to use these terms sloppily.

*Solution 10.2* For a displacement frequency response function it would be counts/ displacement, for a velocity frequency response function it would be counts/velocity, and counts/acceleration for an acceleration frequency response function respectively.

For example for the displacement frequency response function, we have displacement as unit for the input signal, displacement per Hz for the spectrum, counts for the unit of the output signal and counts per Hz for the corresponding spectrum. Since the frequency response function is also defined as the Fourier spectrum of the output signal divided by the Fourier spectrum of the input signal, the unit is counts/displacement.

*Solution 10.3* The velocity impulse response function is the inverse Fourier transform of:

$$T_{vel}(j\omega) = \frac{Output(j\omega)}{Input_{vel}(j\omega)} \quad (10.3-1)$$

a) Displacement impulse response: What we need to know is the response of the system to an input signal given in displacement. By equivalence between differentiation in the time domain and multiplication with  $j\omega$  in the frequency domain, the velocity input spectrum is related to the displacement input spectrum by

$$Input_{vel}(j\omega) = j\omega \cdot Input_{disp}(j\omega) \quad (10.3-2)$$

Hence

$$T_{vel}(j\omega) = \frac{Output(j\omega)}{j\omega \cdot Input_{disp}(j\omega)} \quad (10.3-3)$$

and replacing  $Output(j\omega)/Input_{disp}(j\omega)$  by  $T_{disp}(j\omega)$  we obtain

$$T_{disp}(j\omega) = \frac{Output(j\omega)}{Input_{disp}(j\omega)} = T_{vel}(j\omega) \cdot j\omega \quad (10.3-4)$$

Hence, the displacement frequency response function can be obtained from the velocity frequency response function by multiplication with  $j\omega$ . Again, by equivalence between multiplication with  $j\omega$  in the frequency domain and differentiation in the time domain, the displacement impulse response function is obtained from the velocity impulse response function by differentiation.

b) Acceleration impulse response: By the same argument we obtain the acceleration frequency response function from the velocity response function by division by  $j\omega$ . Finally, by equivalence between division by  $j\omega$  in the frequency domain and integration in the time domain, the acceleration impulse response function can be obtained from the velocity impulse response function by integration.

*Solution 10.4* We can directly use (10.7) with  $\omega_0 = 2\pi \cdot f_0 = 0.0519657$ ,  $h = 0.718$ , and  $G = 1500$  [V/m/s] to obtain the velocity transfer function

$$T_{vel}(s) = -1500[V/m/s] \frac{s^2}{s^2 + 0,07462s + 0,0027} \quad (10.4-1)$$

From the discussion of Problem 10.3 we know that we obtain the displacement response function by multiplication with  $s$ .

$$T_{disp}(s) = -1500[V/m] \frac{s^3}{s^2 + 0,07462s + 0,0027} \quad (10.4-2)$$

The unit of the scale factor in this case becomes [V/m]. We can also express the denominator polynomial by its roots (see equation (10.5)) which are given by equation (10.8)

(  $s_{p(1,2)} = -(h \pm \sqrt{h^2 - 1}) \cdot \omega_0$  ). With the parameters given above we obtain

$$s_{p(1,2)} = -(0,718 \pm 0,696 \cdot j) \cdot 0,0519657 = -(0,03731 \pm 0,03617 \cdot j) \quad \text{and}$$

$$T_{disp}(s) = \frac{-1500 \left[ \frac{V}{m} \right] \cdot s^3}{(s + 0,03731 + j \cdot 0,03617) \cdot (s + 0,03731 - j \cdot 0,03617)} \quad (10.4-3)$$

The corresponding frequency response function is obtained by evaluating  $T(s)$  on the

imaginary axis ( $s \rightarrow j\omega$ ).

$$T_{disp}(j\omega) = \frac{-1500 \left[ \frac{V}{m} \right] \cdot (j\omega)^3}{(j\omega + 0,03731 + j \cdot 0,03617) \cdot (j\omega + 0,03731 - j \cdot 0,03617)} \quad (10.4-4)$$

*Solution 10.5* With an LSB of  $2.5 \mu V$  we obtain the  $1V = 0,4 \cdot 10^6$  counts. Hence  $T_{disp}(j\omega)$  has to be multiplied by  $0,4 \cdot 10^6$  to come out in counts and to be divided by  $10^9$  to convert  $m$  into  $nm$ .

$$T_{disp}(j\omega) = \frac{-0,6 \left[ \frac{cts}{nm} \right] \cdot (j\omega)^3}{(j\omega + 0,03731 + j \cdot 0,03617) \cdot (j\omega + 0,03731 - j \cdot 0,03617)} \quad (10.5-1)$$

The shape of the modulus of the displacement frequency response function for this system is shown in Fig. A 10.5.

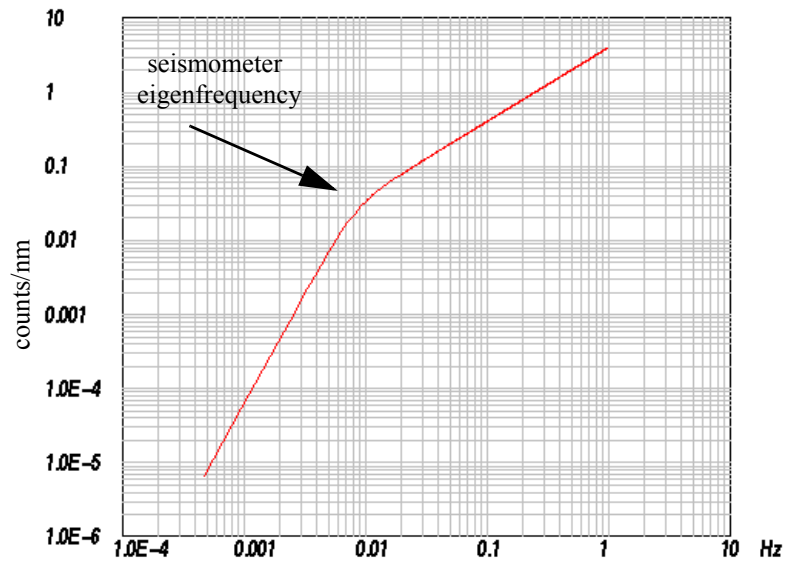


**Fig. A 10.5** Displacement amplitude frequency response function for Problem 10.5. Amplitude in counts/nm.

*Solution 10.6* As discussed in the context of Problem 10.3, the displacement frequency response function can be obtained from the velocity response function by multiplication with  $j\omega$ . Again, by equivalence between multiplication with  $j\omega$  in the frequency domain and differentiation in the time domain, the displacement impulse response function is obtained from the velocity impulse response function by differentiation.

Here we want to go the other way, hence in order to obtain the velocity frequency response function, we have to either calculate the spectrum from the integrated displacement impulse response function or divide the displacement frequency response function by  $j\omega$ . Another way is by removing a zero from the GSE calibration file describing the transfer function. The result is shown in Fig. A 10.6.

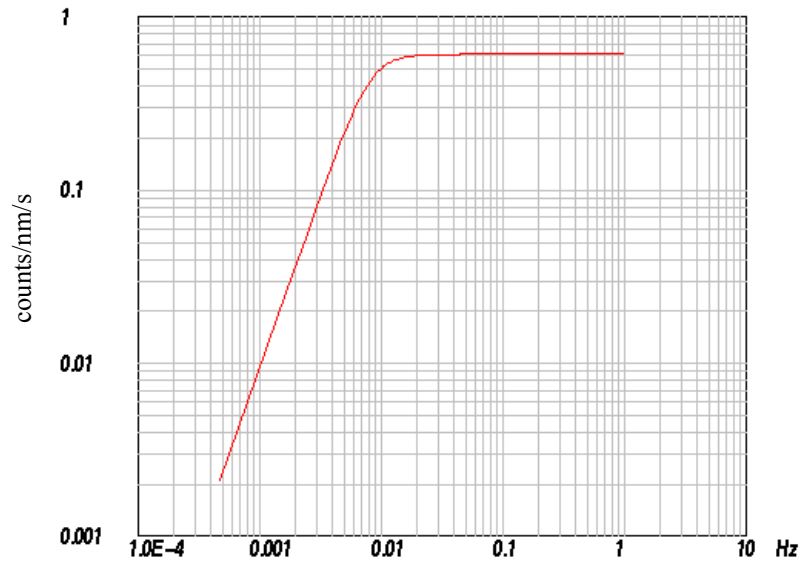


**Fig. A 10.6** Velocity amplitude frequency response function for Problem 10.6. Amplitudes in counts/nm/s.

Note that the plateau value is 0.6 counts/nm/s, which corresponds to the generator constant expressed in counts<sup>1</sup>.

*Solution 10.7* The scale factor in equation (10.11)

$$T(j\omega) = T_{disp}(j\omega) = C_{disp} \cdot \frac{\prod_{k=1}^L (j\omega - s_{0k})}{\prod_{l=1}^L (j\omega - s_{pl})} = C_{disp} \cdot F_{disp}(j\omega) \quad (10.7-1)$$

must be chosen such that  $T_{disp}(j\omega_{cal}) = 1/g_d$ .

Hence we obtain  $1/g_d = C_{disp} \cdot |F_{disp}(j\omega_{cal})|$  which yields

---

1. The systems discussed in Problem 10.4 to Problem 10.6 describes the stations of the German Regional Seismic Network (GRSN) as of June 1994.

$$C_{disp} = 1/(g_d \cdot |F_{disp}(j\omega_{cal})|) . \quad (10.7-2)$$

**Solution 10.8** In the context of the solution of Problem 10.7, we have seen that the scale factor  $C_{disp}$  is calculated as  $C_{disp} = 1/(g_d \cdot |F_{disp}(j\omega_{cal})|)$ . Here,  $g_d$  was defined as  $g_d = A_i^{disp}/A_o$ , with  $A_i^{disp}$  the displacement amplitude of the input signal and  $A_o$  being the amplitude of the output signal in counts. If we are measuring the velocity amplitude of the input signal as in Fig. A 10.7, we get  $g_v = A_i^{vel}/A_o$  or in case of acceleration  $g_a = A_i^{acc}/A_o$ .

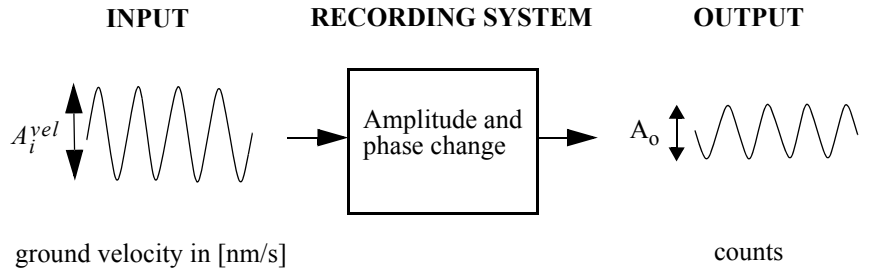


**Fig. A 10.7** Sketch of a shaking table experiment to measure the calibration gain  $g_v$  at a given period.

However, for an harmonic signal at calibration frequency  $\omega_{cal}$ , we obtain  $A_i^{acc} = \omega_{cal} \cdot A_i^{vel} = \omega_{cal}^2 \cdot A_i^{disp}$  and  $A_i^{vel} = \omega_{cal} \cdot A_i^{disp}$ . Therefore, we get

$$g_v = \frac{A_i^{vel}}{A_o} = \frac{\omega_{cal} \cdot A_i^{disp}}{A_o} = \omega_{cal} \cdot g_d \text{ and } g_d = \frac{g_v}{\omega_{cal}}$$

and  $g_d$ . Likewise,  $g_d = \frac{g_a}{\omega_{cal}^2}$ . As a consequence, we obtain for the scale factor

$$C_{disp} = \frac{1}{g_d \cdot |F(j\omega_{cal})|} = \frac{\omega_{cal}}{g_v \cdot |F(j\omega_{cal})|} = \frac{\omega_{cal}^2}{g_a \cdot |F(j\omega_{cal})|} \quad (10.8-1)$$

*Solution 10.9* Since the sensor is supposed to generate a voltage which is proportional to ground velocity for frequencies above 1 Hz, we have a system similar to that described in Solution 10.4 only with different parameters. For  $G = 100 \text{ V/m/s}$ ,  $f_0 = 1.0 \text{ Hz}$  ( $\omega_0 = 6.283$ ), and  $h = 0.7$  the velocity transfer function is

$$T_{vel}(s) = -100 \left[ \frac{V}{m/s} \right] \frac{s^2}{s^2 + 8,7964s + 39,476} \quad (10.9-1)$$

From the discussion of Problem 10.3 we know that we can calculate the displacement response function by multiplication with  $s$

$$T_{disp}(s) = -100 \left[ \frac{V}{m} \right] \frac{s^3}{s^2 + 8,7964s + 39,476} \quad (10.9-2)$$

The unit of the scale factor in this case becomes [V/m]. We can express the denominator polynomial by its roots (see equation (10.5)) which are given by equation (10.8)

(  $s_{p(1,2)} = -(h \pm \sqrt{h^2 - 1}) \cdot \omega_0$  ). With the parameters given above we obtain

$$s_{p(1,2)} = -(0,7 \pm j \cdot 0,71414) \cdot 6,283 = -(4,398 \pm j \cdot 4,487) \quad (10.9-3)$$

As in Solution 10.4 we can use equation (10.5) with these 2 poles and three zeros at the origin and the fact that  $\beta_L = 100 \text{ [V/m]}$  and  $\alpha_N = 1$ , hence  $(\beta_L/\alpha_N) = 100 \text{ [V/m]}$  in (10.5). However, since the signal is amplified by 250 before being fed into the A/D converter, we must be aware that the effective factor  $\beta_L$  is  $100 \cdot 250 = 2,5 \cdot 10^4$ . For the frequency response function (evaluating  $T(s)$  for  $s = j\omega$ ) relating output voltage and ground displacement we obtain

$$T_{disp}(j\omega) = \frac{-2,5 \cdot 10^4 \left[ \frac{V}{m} \right] \cdot (j\omega)^3}{(j\omega + 4,398 + j \cdot 4,487) \cdot (j\omega + 4,398 - j \cdot 4,487)} \quad (10.9-4)$$

With an LSB of  $1 \mu V$  we obtain  $1 V = 10^6$  counts. Hence  $T_{disp}(j\omega)$  has to be multiplied by  $10^6$  to come out in counts and to be divided by  $10^9$  to convert  $m$  into  $nm$ .

$$T_{disp}(j\omega) = \frac{-25 \cdot \left[ \frac{counts}{nm} \right] \cdot (j\omega)^3}{(j\omega + 4,398 + j \cdot 4,487) \cdot (j\omega + 4,398 - j \cdot 4,487)} \quad (10.9-5)$$

Following the argument in Solution 10.6, we obtain the velocity frequency response function by dividing the displacement frequency response function by  $j\omega$ .

$$T_{vel}(j\omega) = \frac{-25 \cdot \left[ \frac{counts}{nm} \right] \cdot (j\omega)^2}{(j\omega + 4,398 + j \cdot 4,487) \cdot (j\omega + 4,398 - j \cdot 4,487)} \quad (10.9-6)$$

In order to obtain  $g_d = 1/|T_{disp}(j\omega_{cal})|$  and  $g_v = 1/|T_{vel}(j\omega_{cal})|$ , we have to evaluate the modulus of the displacement frequency response function and the velocity response function at the calibration frequencies. Calculating these values (using a pocket calculator) and  $f_{cal} = \omega_{cal}/2\pi$  of 5 and 10 Hz, respectively, we obtain:

$$5 \text{ Hz: } g_d = 0,00127324 \text{ [nm/counts]} \text{ and } g_v = 0,03999 \text{ [nm/s/counts]}$$

$$10 \text{ Hz: } g_d = 0,00063652 \text{ [nm/counts]} \text{ and } g_v = 0,03999 \text{ [nm/s/counts]}.$$

From Solution 10.8 we know that for harmonic input signals with signal frequency equal to the calibration frequency we obtain  $g_d = A_i^{disp}/A_o$  and  $g_v = A_i^{vel}/A_o$ . Hence the frequency response function at the calibration frequency should be  $A_o = A_i^{disp}/g_d$  and  $A_o = A_i^{vel}/g_v$ .

In Fig. A 10.8, the displacement frequency response function has been calculated using DST for the two poles at  $4,398 \pm 4,487$ , three zeros at the origin and a scale factor of 25 (internal sampling frequency 50 Hz, window length 4096).

So for the following argument  $A_i = 1,0$ . At 5 Hz, we expect  $A_o = A_i^{disp}/g_d = 1,0/0,00127324 = 785$  [counts]. Likewise at 10 Hz we obtain  $A_o = 1571$  [counts] which can be seen to be the case in Fig. A 10.8.

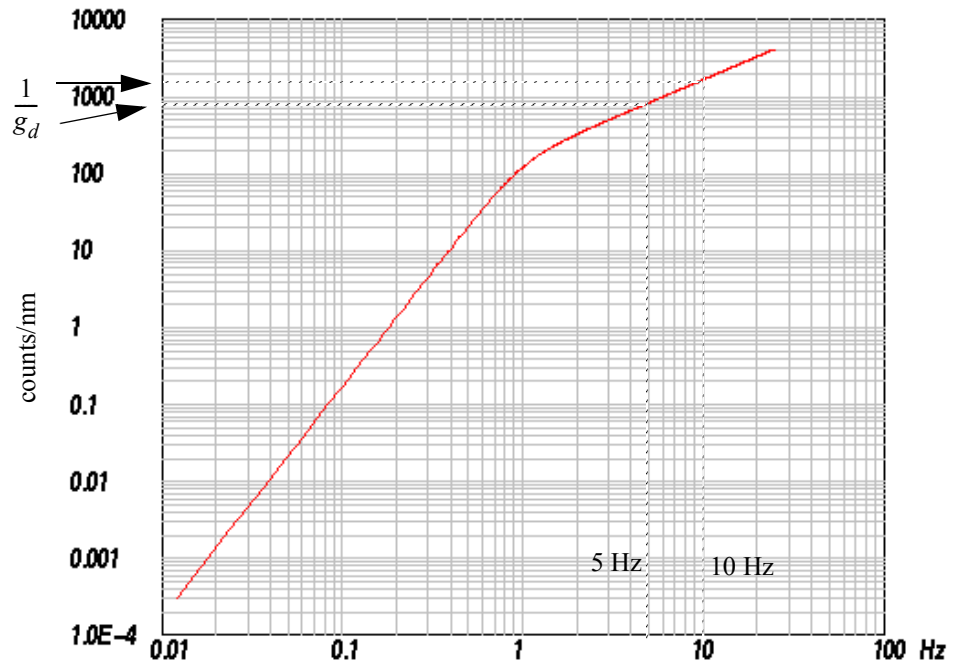


**Fig. A 10.8** Displacement amplitude frequency response function for Problem 10.9.

In Fig. A 10.9, the velocity frequency response function is displayed. It has been calculated the same way as the displacement frequency response function except for the fact that one of the zeros has been removed in order to account for the differences between displacement and velocity frequency response function.

From the same argument as for the displacement frequency response at 5 Hz, we expect  $A_o = A_i^{vel}/g_v = 1,0/0,03999 = 25$  counts and the same value as for 10 Hz. We see in Fig. A 10.9 that both calibration frequencies are within the flat portion of the velocity frequency response function.

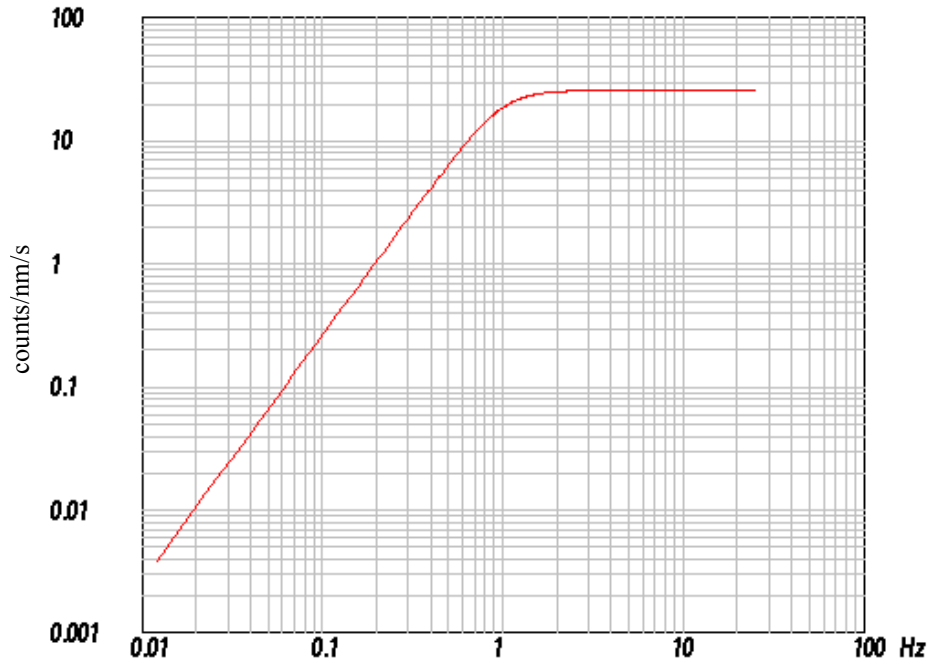


**Fig. A 10.9** Velocity amplitude frequency response function for Problem 10.9.

*Solution 10.10* Since the signal is a harmonic signal, all we have to do is determine the magnification in [counts/nm] for ground displacement at the signal frequency and divide the peak-to-peak amplitude in counts by that factor. Since we have 5 oscillations within 1 sec, the signal frequency is 5 Hz. We have already calculated the magnification at that frequency (Solution 10.9). For the peak-to-peak amplitude of 396 counts, we therefore obtain the peak-to-peak displacement amplitude as:

$$396 / |T_{disp}(j \cdot 2\pi f)|_{f=5\text{Hz}} = 396 \cdot g_d^{5\text{Hz}} = 396 \cdot 0,00127324 = 0,5042\text{nm} \quad .$$

*Solution 10.11* Because the resulting filter is causal, there is no signal before the sample corresponding in time to the input 'spike'. As a consequence, the zero crossings of the harmonic components at the Nyquist frequency must remain exactly at sample intervals. Therefore, the corresponding phase delay at the Nyquist frequency must be an multiple of the sampling interval, which necessarily causes a distortion of the phase response.

*Solution 10.12* Because the slope of a sinusoid  $A_0 \cdot \sin(\omega t)$  equals  $\omega \cdot A_0 \cdot \cos(\omega t)$ ,  $slope_{max} = \omega \cdot A_0$ , and with  $a_{max} = 2A_0$  the rise time for a sinusoid becomes

$$t_{r(\text{sinusoid})} = 2/\omega = 2/(2\pi \cdot f) = T/\pi \quad (10.12-1)$$

with  $T$  the period of the sinusoid. Hence, for a sinusoidal signal, the rise time and the duration as measured from the time difference between zero crossings are related by a constant factor of  $\pi$ .

*Solution 10.13* In Fig. A 10.10 the input spike, the causal and the acausal impulse responses of the 8 pole (4 section), 1 Hz Butterworth LP filter are displayed.

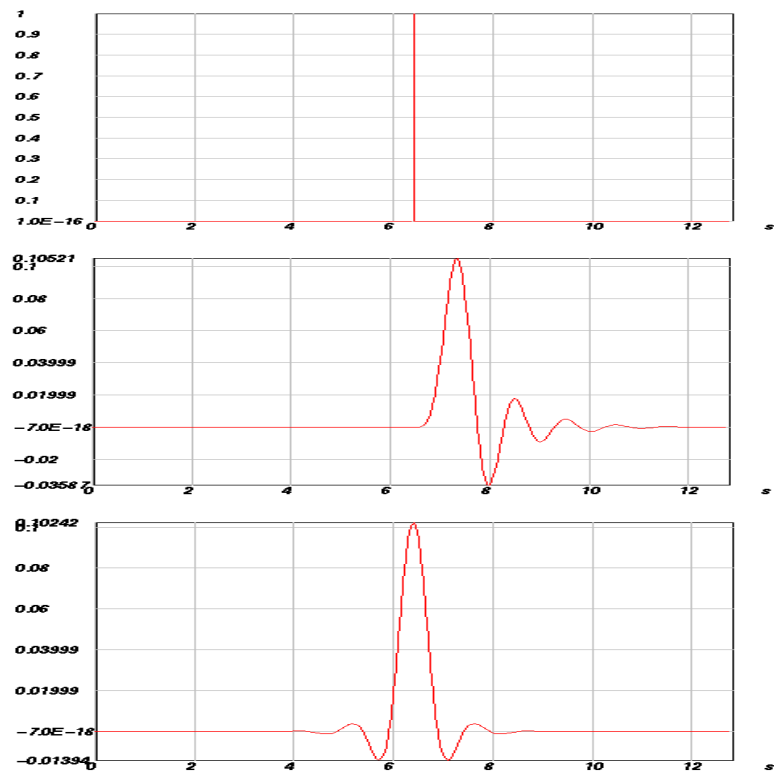


**Fig. A 10.10** Input spike, the causal and the acausal impulse response of the 8 pole (4 section) Butterworth filter (from top to bottom)

In contrast to the acausal filter, the causal filter shows a delay of both the maximum amplitude and the onset. For the acausal filter, the maximum amplitude is not delayed.

Several properties can be noted. For the causal filter, the onset shows the change in the onset order which slightly enlarges the pulse duration as measured from zero crossings with respect to the acausal filter. Remember that for the acausal filter the definition of an onset makes no sense. While the oscillations in the impulse response of the causal filter have larger amplitudes the frequencies are the same. Similar effects are visible for the step response function in Fig. A 10.11. Since the maximum values of the impulse response functions are very close, the maximum slopes of the step response functions and the rise times will be similar as well. Nevertheless, visually we note an apparent increase in the rise time for the causal filter, again caused by the change of the onset order.

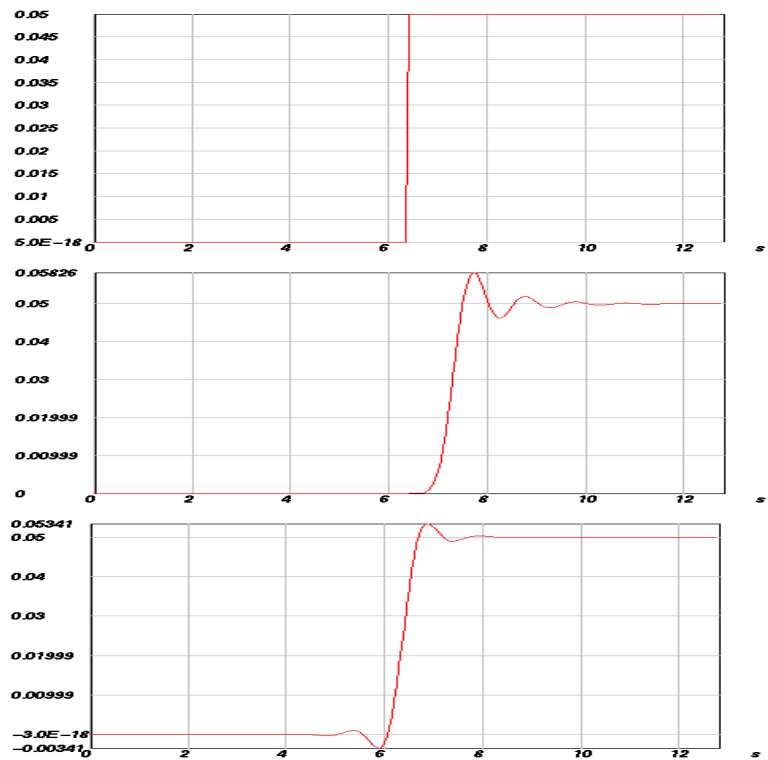


**Fig. A 10.11** Superimposed step response functions for the 8 pole, 1Hz Butterworth LP filter for the causal and acausal case.